Threshold phenomena in nuclear reactions

S. N. Abramovich, B. Ya. Guzhovskiĭ, and L. M. Lazarev
All-Union Institute of Experimental Physics, Arzamas-16

Phys. Elem. Chastits At. Yadra **23**, 305–363 (March–April 1992)

Progress in the study of threshold phenomena during the last two decades is reviewed. It is shown that anomalous behavior of the excitation function near the reaction thresholds is a typical phenomenon and is observed in nuclear reactions for all nuclei. Feshbach's theory of nuclear reactions has been significantly developed for the description of threshold phenomena. The resonating-group method has been widely used in various modifications for this purpose. The possibilities for determining parameters and properties of a nuclear system as a result of analysis of complete and incomplete experiments are studied. Problems of multiparameter analysis of experimental data are discussed. The most interesting experimental data are analyzed. Unresolved problems in the theory and analysis of threshold phenomena are formulated.

INTRODUCTION

Threshold phenomena in nuclear reactions have already attracted the attention of physicists for almost half a century because of the unique possibility that they offer for detailed study of nuclear structure near the energy threshold for production of new particles or the opening of new reaction channels. In the region of a threshold, the energy dependence of the physical quantities changes abruptly because of the radical internal rearrangement of the nuclear system.

After Wigner's pioneering theoretical study in 1948 of threshold phenomena,[1] there were some experimental studies[2] that stimulated further development of the theoretical description of threshold irregularities in the scattering and reaction cross sections. Breit[3] investigated the energy dependence of the cross section near the threshold for production of two charged particles. Baz' proposed[4] principles for extending the theory to an open channel in the region of a two-particle neutral-particle production threshold. The early theoretical studies[1,3,4] were based on R-matrix theory, and their results are applicable to problems with one open channel and one resonance. The theory of threshold phenomena then developed along several directions based on different approaches: 1) R-matrix theory; 2) Feshbach's unified theory of nuclear reactions;[5] 3) the resonating-group method;[6] 4) analytic S-matrix theory;[7] 5) dispersion theory of nuclear reactions.[8] Three approaches are based on the microscopic Schrödinger equation; the last two use the analytic properties and unitary of the S matrix. The first two approaches determined the direction in the development of model-free theory, the main aim of which is to find the energy dependence of the system's wave function and a parametrization of it in the space of reaction channels. In low-energy physics and in the framework of model-free theory, requirements for a complete experiment were successfully formulated,[4,9] and it was shown that it is in principle possible to determine the parameters and to recover the wave function in the subspace of reaction channels. Approaches 3–5 facilitated the development of model threshold theories to make it possible to calculate physical quantities with good accuracy. Comparison of the results of analysis of experimental data by model-free and model theories is a good test of the validity of the theories and a stimulus for further development of investigations of threshold phenomena.

A task of primary importance is the accumulation of new fully reliable experimental data. As a rule, the existing data are not sufficiently accurate or complete, and it is only for nuclei with $A=4$–8 that the experimental data are suitable for systematic analysis, although they are not sufficiently complete.

Threshold irregularities are most clearly expressed in reactions of $1p$-shell nuclei. This review is devoted to a description of the investigations of the threshold states of these nuclei. In Sec. 1 we analyze the known data on light-nucleus levels and find about a hundred neutron thresholds with low-lying compound-nucleus levels. These energy-correlated threshold–resonance state pairs have several properties typical of them all. Threshold states without a neighboring resonance are encountered less often (10–20% of the cases) and exhibit a greater diversity of properties. For medium and heavy nuclei, it is more difficult to trace the behavior near thresholds; however, here too, anomalous behavior of the cross sections is observed in the region of thresholds of analog channels. In Sec. 2, we present the existing theoretical approaches to the analysis of the experimental data with their advantages and shortcomings. The fullest exposition is of the application of Feshbach's unified theory to threshold phenomena, by means of which the authors of this review have analyzed experimental data. In Sec. 3, the complete-experiment problem is considered, and its solution used to determine the volume of physical information that can be obtained from an "incomplete" experiment in which the integrated excitation function and the excitation function at a certain angle are measured. Requirements on the experimental data are also formulated. In Sec. 4, we discuss some problems of multiparam-

 0090-4759/92/020129-27$04.00

eter least-squares description of experimental excitation functions near a threshold. In. Sec. 5 we present the results of analysis of experimental data. Open problems of theory and experiment in threshold regions are formulated in Sec. 6. In conclusion we summarize the theoretical and experimental investigation of threshold phenomena.

The review is based on experimental and theoretical studies made by colleagues at the All-Union Institute of Experimental Physics during the last decade. The aim of the review is to describe the general status of threshold investigations at the present time and to characterize the main tendencies and directions in the development of these investigations.

1. UBIQUITY OF THRESHOLD SITUATIONS IN NUCLEI

We give some definitions that will be used in the paper. We define a *threshold state* of a nucleus as a state at energy equal to the threshold energy for the opening of a new reaction channel. A *threshold level* of a nucleus is a resonance state of it lying in the neighborhood of a threshold at a distance of the order of the level width. The number of threshold levels can be high for high level densities and large widths. A *resonance threshold state* is a threshold state near a resonance of a nucleus. We now show that the number of threshold states and threshold levels is large. Their study opens up a wide field of activity. Light-nucleus levels near neutron decay thresholds, $A \to (A-1)+n$, have been analyzed. Threshold situations in which a neutron threshold state is a resonance have been selected. The selection criterion were: 1) the level of nucleus A is within a distance of the level width of the threshold, $|E^{J\pi}-E_q| < \Gamma^{J\pi}$, where $E^{J\pi}$ and $\Gamma^{J\pi}$ are the energy and width of the level, which has spin J and parity π; E_q is the threshold energy; 2) the threshold and resonance states have similar structure (large partial reduced width γ_n^2); 3) the final nucleus $A-1$ in the threshold channel has a long life, i.e., its width is $\Gamma^{I\pi} < \Gamma^{J\pi}$, where I is the spin of the nucleus $A-1$.

Several tens of threshold situations satisfying criteria 1–3 were found[10] in the mass range $A=4$–18. They are given in Table I, which gives properties of the nuclei A and $A-1$, and also the minimum neutron orbital angular momentum l in the threshold channel, the neutron-decay threshold energy E_q of the nucleus A, and $\Delta E = E^{J\pi}-E_q$.

It can be seen from Table I that in the majority of cases the neutron thresholds are at nuclear excitation energies 10–20 MeV, and the minimum neutron orbital angular momentum is zero. Neutron threshold levels have isospin in the interval $T=0$–2. Levels with higher isospin are evidently at higher excitation energies. The correlations in Table I between the thresholds and the threshold levels of the nuclei together with the structural similarity of neighboring threshold anomalies in the ^{7}Li$(t, p)^9$Li reaction excitation function in the region of two thresholds of the ^{7}Li$(t, n)^9$Be$^*(T=3/2)$ reaction[11–13] and in the ^{7}Li$(^3$He, $p)^9$Be reaction excitation function near two thresholds of the ^{7}Li$(^7$He, $n)^9$Be$(T=3/2)$ reaction[14] showed that the isobaric multiplet with $A=10$ and isospin $T=2$ has a topological system of neutron threshold levels, i.e., states with the same quantum numbers and related structure. Moreover, analysis of the two threshold anomalies in the ^{10}Be$(\alpha, p)^{13}$B reaction excitation function[15] near two neutron thresholds of the ^{10}Be$(\alpha, n)^{13}$C$(T=3/2)$ reaction showed that the quantum numbers of the two ^{14}C$(T=2)$ threshold levels are the same as in the $A=10$ multiplet. The strong-interaction isobaric invariance[16] suggests that the isobaric $A=14$ multiplet with $T=2$ will have properties similar to those of the $A=10$ multiplet with $T=2$, especially since the nuclei of these multiplets belong to the p-shell nuclei. The data of Table I indicate that the threshold levels of the isobaric $A=18$ multiplet with $T=2$ have the same quantum numbers. The $\Delta A=4$ periodicity noted here in the properties of the threshold states and threshold levels is also suggested for isobaric multiplets with other A and T. This is indicated by the quantum numbers of the levels in Table I for the compound and the residual nucleus:

$$^{11}\mathrm{B}(1^+/2,3/2) \to {}^{10}\mathrm{B}(0^+,1)+n,$$

$$^{15}\mathrm{N}(1^+/2,3/2) \to {}^{14}\mathrm{N}(0^+,1)+n.$$

The limited data on light-nucleus levels does not permit further comparisons and analogies.

The pair correlation of threshold states and threshold levels can be fortuitous at a high density of thresholds and resonance states. This makes it difficult to look for dependences exhibited with increasing mass number A due to the strong suppression of the threshold irregularities of the resonance structure in the excitation function. However, here too anomalous behavior of the cross sections is observed in the region of thresholds of analog reaction channels. Typical threshold irregularities can be seen[17] in the cross sections for elastic and inelastic scattering of protons by nuclei with masses $A=23$–35 near the (p, n) reaction threshold. These nuclear processes involve production of a compound nucleus. Threshold effects have also been discovered in direct (d, p) reactions near the neutron threshold.[18] Return to a situation with rare resonances and thresholds is possible in medium-heavy nuclei if isobar analog resonances are studied near (p, n) reaction thresholds, when the averaging over the continuum of resonances with $T_<$ leads to a smooth energy dependence of the cross sections far from the isobar analog resonances.[19] Threshold anomalies have been observed in the cross sections of direct nuclear (d, p) reactions on nuclei with masses $A=90$–210 near the (d, n) reaction threshold with excitation of analog states.[19,20]

In recent years, the discovery of threshold phenomena has been extended to fissioning nuclei. Analysis[21,22] of the fissilities and fission-fragment angular distributions of some isotopes of thorium, uranium, and plutonium in (d, pf), (t, pf), and (n, nf) reactions showed that in the fission channel at excitation energies 5–8 MeV, or even–even nuclei at least, there are intermediate states that are correlated, within their widths, with neutron thresholds for the

TABLE I. Data on levels of the compound nucleus A and final nucleus $A-1$ in the neutron channel near the $A \rightarrow (A-1)+n$ decay threshold.

Nucleus A	E, MeV	J^π, T	Γ, keV	$A-1$ (final nucleus + particle)	E, MeV	J^π, T	Γ, keV	l	E_q, MeV	ΔE, keV
^{4}He	20,1	0^+; 1	270	^{3}H + p	0	$1^+/2$; 1/2	0	0	19,8	300
				^{3}He + n	0	$1^+/2$; 1/2	0	0	20,6	−500
^{5}He	16,760	$3^+/2$; 1/2	100	^{3}H + d	0	$1^+/2$; 1/2	0	0	16,696	64
^{6}He	1,797	$(2)^+$; 1	113	^{5}He + n	0	$3^-/2$; 1/2	600	1	1,87	−73
^{5}Li	16,657	$3^+/2$; 1/2	300	^{3}He + d	0	$1^+/2$; 1/2	0	0	16,387	270
^{6}Li	4,31	2^+; 0	1,700	^{5}He + p	0	$3^-/2$; 1/2	600	1	4,593	−283
	5,366	2^+; 1	540	^{5}Li + n	0	$3^-/2$; 1/2	1500	1	5,666	−300
	5,65	1^+; 0	1,500	^{5}Li + n	0	$3^-/2$; 1/2	1500	1	5,666	−16
^{7}Li	7,460	$5^-/2$; 1/2	89	^{6}Li + n	0	1^+; 0	0	1	7,250	210
	9,67	$7^-/2$; 1/2	400	^{6}Li + n	2,185	3^+; 0	0,024	1	9,435	235
	9,85	$3^-/2$; 1/2	1200	^{6}He + p	0	0^+; 1	0	1	9,975	−125
	11,24	$3^-/2$; 3/2	260	^{6}Li + n	3,562	0^+; 1	0	1	10,812	428
^{8}Li	2,255	3^+; 1	33	^{7}Li + n	0	$3^-/2$; 1/2	0	1	2,033	222
	3,21	1^+; 1	1000	^{7}Li + n	0,478	$1^-/2$; 1/2	0	1	2,511	701
^{6}Be	1,67	$(2)^+$; 1	1160	^{5}Li + p	0	$3^-/2$; 1/2	1500	1	0,59	−1080
^{7}Be	7,210	$5^-/2$; 1/2	500	^{6}Li + p	0	1^+; 0	0	1	5,606	1604
	9,27	$7^-/2$; 1/2	—	^{6}Li + p	0	3^+; 0	0,024	1	7,791	1479
	9,9	$3^-/2$; 3/2	1800	^{6}Be + n	0	0^+; 1	92	1	10,676	−776
	11,01	$3^-/2$; 3/2	320	^{6}Li + p	3,562	0^+; 1	0	1	9,168	1842
^{8}Be	16,626	2^+	108	^{7}Li + p	0	$3^-/2$; 1/2	0	1	17,254	−628
	16,922	2^+	74	^{7}Li + p	0	$3^-/2$; 1/2	0	1	17,254	−332
	17,64	1^+; 1	107	^{7}Li + p	0,478	$1^-/2$; 1/2	0	1	17,732	−92
	18,15	1^+; 0	138	^{7}Li + p	0,478	$1^-/2$; 1/2	0	1	17,732	418
	18,912	2^-	57	^{7}Be + n	0	$3^-/2$; 1/2	0	0	18,898	12
	19,055	3^+; 1	294	^{7}Be + n	0	$3^-/2$; 1/2	0	1	18,898	172
	19,218	3^+; 0	203	^{7}Be + n	0	$3^-/2$; 1/2	0	1	18,898	342
	19,399	1^-	640	^{7}Be + n	0,429	$1^-/2$; 1/2	0	0	19,327	63
^{9}Be	1,685	$1^+/2$; 1/2	150	^{8}Be + n	0	0^+; 0	0	0	1,665	20
^{9}Be	2,429	$5^-/2$; 1/2	0,77	^{5}He + α	0	$3^-/2$; 1/2	600	2	2,46	−31
	16,975	$1^-/2$; 3/2	0,47	^{7}Li + d	0	$3^-/2$; 1/2	0	0	16,696	279
	17,298	$5^-/2$	200	^{8}Li + p	0	2^+; 1	0	1	16,887	411
	17,493	$7^+/2$; 1/2	47	^{6}Li + t	0	1^+; 0	0	2	17,688	−195
	18,02	—	—	^{6}Li + t	0,981	1^+; 1	0	—	17,868	252
	18,58	—	—	^{6}Li + t	0	1^+; 0	—	—	17,688	892
^{10}Be	9,27	(4^-); 1	150	^{9}Be	2,429	$5^-/2$	0,8	2	9,241	30
	9,4	2^+; 1	291	^{9}Be	3,049	$5^+/2$	282	0	9,861	−460
^{11}B	11,589	$5^+/2$	170	^{10}B	0	3^+; 0	0	0	11,454	140
^{11}B	12,557	$1^+/2$; 3/2	210	^{10}B	1,740	0^+; 1	0	0	13,194	−640
	13,16	$5^+/2$; −	430	^{10}B	2,154	1^+; 0	0	2	13,608	−448
	15,32	$5^+/2$; 3/2	635	^{10}B	3,587	2^+; 0	—	0	15,041	280
	18,37	(1/2; 3/2; 5/2)$^+$	260	^{10}B	7,002	$(1;2)^+$;0	100	0	18,458	−86

TABLE I. (*Continued.*)

Nucleus A	E, MeV	J^π, T	Γ, keV	$A-1$ (final nucleus + particle)	E, MeV	J^π, T	Γ, keV	l	E_q, MeV	ΔE, keV
^{12}B	3,388	3^-; 1	0	^{11}B	0	$3^-/2$; 1/2	0	2	3,370	18
^{13}C	14,390	$(5^-/2)$	280	^{12}C	9,641	3^-	34	0	14,597	−207
^{14}C	11,306	1^+	46	^{13}C	3,089	$1^+/2$; 1/2	0	0	11,266	40
^{14}N	10,540	1^-	140	^{13}N	0	$1^+/2$; 1/2	0	0	10,553	−13
	14,250	3^+; 0	420	^{13}N	3,547	$5^+/2$; 1/2	47	0	14,100	150
	18,1	4^+	600	^{13}N	7,155	$7^+/2$; 1/2	9	0	17,708	400
	18,2	3^-	400	13N	7,356	$5^-/2$; 1/2	75	0	17,929	270
	20,1	1^-	500	13N	9,476	$3^-/2$; 1/2	30	0	20,029	70
	20,8	3^-	500	13N	10,36	$(5/2, 7/2)^-$	76	0	20,913	−113
	22,5	2^-; 1	—	^{13}N	11,700	$5^-/2$	115	0	22,253	250
^{15}N	10,804	$3^+/2$	10	^{14}N	0	1^+; 0	0	0	10,833	−30
	11,615	$1^+/2$; 3/2	405	^{14}N	2,313	0^+; 1	0	0	13,146	−1500
	17,67	$3^+/2$; 1/2	600	^{14}N	7,028	2^+; 0	0	0	17,861	−190
	20,5	$3^+/2$	400	^{14}N	9,703	1^+; 0	15	0	20,536	−36
	25,5	3/2; (3/2)	—	^{14}N	14,66	2	100	0	25,493	7
^{16}N	7,637	$(3)^+$	7	^{15}N	5,270	5/2	0	0	7,761	−120
^{16}N	9,459	≥2	100	^{15}N	7,155	5/2	0	(0)	9,646	−186
	10,055	≥3	30	^{15}N	7,567	7/2	0	0	10,058	0
	11,716	(1^-); 2	12	^{15}N	9,225	1/2	0	0	11,716	0
^{17}O	10,168	$7^-/2$	49	^{16}O	6,130	3^-; 0	0	0	10,274	−110
	10,913	$5^+/2$	42	^{16}O	6,917	2^+; 0	0	0	11,061	−150
	11,079	$1^-/2$; 3/2	2,4	^{16}O	7,117	1^-; 0	0	0	11,261	−180
	12,998	$5^-/2$; 3/2	2,5	^{16}O	8,872	2^-; 0	0	0	13,016	−18
	15,10	$(9^+/2; 1/2)$	500	^{16}O	11,096	4^+; 0	0,3	0	15,240	−140
^{18}O	8,216	2^+	1	^{17}O	0	$5^+/2$	0	0	8,044	170
	13,1	1^-	700	^{17}O	4,552	$3^-/2$	40	0	12,596	100
	13,8	1^-	600	^{17}O	5,939	$1^-/2$	32	0	13,983	−180
	14,7	1	800	^{17}O	6,862	$1^-/2$	<1	0	14,906	−200
	15,8	1^-	700	^{17}O	7,99	$1^-/2$	270	0	16,034	−230
	16,38	(1^-); 2	30	^{17}O	8,20	3/2	60	0	16,244	140
	17,3	1^-; 2	600	^{17}O	9,147	$1^-/2$	4	0	17,191	110
				^{17}O	9,42	$3^-/2$	120	0	17,464	−164

given nucleus and neighboring isotopes. These numerous correlations (10 in number) are hardly fortuitous and indicate a similarity of the threshold states and threshold levels in the fissioning nuclei.

The data considered here reveal a rich diversity of neutron threshold situations in nuclei. If our ambit is extended to thresholds for charged-particle production, the number of threshold situations is considerably multiplied. However, they are difficult to study for two reasons—the intensity is suppressed by the Coulomb barrier, and the energy dependence is complicated.[3,4] Threshold states and levels in light nuclei are the most favorable for study.

2. THEORY OF THRESHOLD PHENOMENA

There are several known theoretical approaches to the description of threshold nuclear states and levels and also threshold singularities in scattering and reaction cross sections. In low-energy physics, theories based on a microscopic Schrödinger equation have been widely used. Wig-

ner's R-matrix approach has been most fully developed (Refs. 1, 3, 4, 23, and 24). The limitation in practice of this approach to single-channel and single-resonance problems stimulated the development of a different approach based on Feshbach's unified theory of nuclear reactions.[5] One of the present authors (Lazarev) has extended the model-free theory of threshold phenomena[9,11,12,25] to threshold situations with arbitrary number of resonances and reaction channels, including many-particle channels. The resonating-group method, proposed by Filippov,[6] and also by Hoffman,[26] is widely used to study threshold states and levels in model calculations.

We shall also briefly describe the application of field-theory methods to threshold phenomena in low-energy physics in the form of analytic S-matrix theory and dispersion theory.

R-matrix theory

In all forms of R-matrix theory (Kapur–Peierls[27]) it is necessary to have a complete system of formal states of all particles; this system is determined in the volume of the nucleus by imposing certain boundary conditions on the surface of the volume. The main advantage of the formulation proposed by Wigner is that it leads to an explicit dependence of all expressions on the energy. This is achieved with energy-independent boundary conditions. The energy dependence of the elements of the R matrix is expressed in the simple form

$$R_{cc'}(E)=\sum_{\lambda}\frac{\gamma_{\lambda c}\gamma_{\lambda c'}}{E_\lambda-E}, \tag{1}$$

where λ labels the complete system of states. The amplitudes $\gamma_{\lambda c}$ of the reduced widths and the energy eigenvalues E_λ in the states λ do not depend on the energy but do depend on the channel radius a_c and the boundary condition B_c. The indices c and c' label the entrance and exit reaction channels. The simplicity of the analytic form of the R-matrix elements is a consequence of probability conservation, the time reversal principle and, apparently, the causality principle.[23] However, the connection between the R-matrix and the collision matrix U, which directly determines the reaction cross section, is rather complicated:

$$\begin{aligned}
&U=\Omega W\Omega, \quad W=1+\mathscr{P}^{1/2}(1-RL^0)^{-1}R\mathscr{P}^{1/2}w,\\
&\Omega_c^+ +\exp\{i(\omega_c-\Phi_c^+\}, \quad \Phi_c^+=\arctan(F_c/G_c),\\
&\omega_c=\sigma_l-\sigma_0=\sum_{n=1}^{l}\arctan(\eta/n), \quad \eta=Z_1Z_2e^2\mu/\hbar^2k,\\
&\mathscr{P}_c^+=P_c^+=[\rho_c/(F_c^2+G_c^2)]_{r_c=a_c}, \quad k_cr_c=\rho_c, \quad w_c^+=2i,\\
&L_c=(\rho_cO_c'/O_c)_{r_c=a_c}=S_c+iP_c,\\
&O_c^+=(G_c+iF_c)\exp(-i\omega_c),\\
&L^0=L-B, \quad S_c=[\rho_c(F_cF_c'+G_cG_c')/(F_c^2+G_c^2)]_{r_c=a_c}.
\end{aligned} \tag{2}$$

Here, the superscript + indicates positivity of the energy in the channel; k is the wave number; Z_1 and Z_2 are the charges; μ is the reduced mass; η is the Coulomb parameter; F_c and G_c are the solutions of the Schrödinger equation for the relative motion of the two nuclei in channel c that are regular and singular at the origin, respectively; B is a real diagonal matrix of the boundary conditions B_c; O_c' is the derivative of the function O_c with respect to r. The diagonal matrices Ω, $\mathscr{P}$, L, and w are defined on the channel surface.

Because of the difficulty of inverting the matrix $1-RL^0$, the expression (2) is unsuitable for practical applications if more than two channels are open (the order of the matrix is equal to the number of channels).

The derivation of the energy dependence of the collision matrix (2) and of the cross sections near threshold proposed by Wigner[1] is made under the assumption $\rho\ll 1$; in the case of charged particles, the condition $\eta\gg 1$ must also be used. The derivation does not use the approximation of an isolated level; however, it proceeds from the requirement that the interval of variation of the energy be much less than the distance to the following level of the compound nucleus. The problem of finding the energy dependence near the threshold is greatly facilitated by the fact that the operator $|1-RL^0|^{-1}$ in the collision matrix (2) is essentially constant for all channels in a region in which there are no compound-nucleus resonances. The cross section for production of particles in the threshold channel (the reaction energy Q is negative) depends on the energy as follows:[1]

$$\begin{aligned}
&\sigma_{cc'}\sim k_{c'}^{2l'+1}, \quad \eta=0,\\
&\sigma_{cc'}\sim\exp(-2\pi\eta_{c'}), \quad \eta>0,\\
&\sigma_{cc'}\sim 1, \quad \eta<0.
\end{aligned} \tag{3}$$

If the entrance channel is a threshold channel ($Q>0$), the energy dependence of the cross sections can be obtained from (3) by the substitution $c'\to c$, $k_{c'}\to k_c$ with multiplication of the cross sections by k_c^{-2}.

In the case of elastic scattering of slow particles,[1]

$$\begin{aligned}
&\sigma_{cc'}\sim k_c^{2l+2l'}, \quad \eta=0,\\
&\sigma_{cc'}\sim k_c^{-2}\exp(-4\pi\eta_c), \quad \eta>0,\\
&\sigma_{cc'}\sim k_c^{-2}, \quad \eta<0.
\end{aligned} \tag{4}$$

If there is an isolated resonance level near a threshold, then[23]

$$|W_{cc'}|^2=\frac{\Gamma_{\lambda c}\Gamma_{\lambda c'}}{(E_\lambda+\Delta_\lambda-E)^2+\Gamma_\lambda^2/4}, \tag{5}$$

where an energy dependence is now contained in the widths $\Gamma_{\lambda c}$ through the penetrability factors P_c^+ (2):

$$\begin{aligned}
&\Gamma_{\lambda c}=2P_c^+\gamma_{\lambda c}^2, \quad \Gamma_\lambda=\sum_c\Gamma_{\lambda c}, \quad \Delta_\lambda=\sum_c\Delta_{\lambda c},\\
&\Delta_{\lambda c}\approx -S_c^0\gamma_{\lambda c}^2, \quad S_c^0=S_c-B_c.
\end{aligned} \tag{6}$$

Thus, possibilities for determining the energy dependence of the cross section near a threshold in R-matrix theory are limited to a small number of situations in which not more than two reaction channels are open and there is not more

than one isolated compound-nucleus resonance near the threshold. In all the more complicated situations, it is necessary to seek simplifying assumptions. Three-particle decay can be described only if it takes place in two stages: $a+X\to b+Y^*\to b+c+d$. Another shortcoming of the theory is the fact that not all parameters have a transparent physical meaning.

Unified theory of nuclear reactions

We describe the theory in the projection-operator representation, in which the main results can be most succinctly formulated. Thus, for the system of A nucleons we consider the microscopic Schrödinger equation

$$(E-\hat{H})\Psi(r_1,r_2,...,r_A)=0. \tag{7}$$

The variables r_k include the spatial coordinate, spin, and isotopic spin; $\hat{H}$ is the Hamiltonian of the system.

In the complete space of many-particle states of the A-nucleon system, we separate the subspaces of open reaction channels. The subspaces contain the states $|j,\ m\rangle$, which describe the internal motion of two clusters, m and $A-m$, characterized by the set of quantum numbers j. Each of the clusters may consist of a single nucleon. A cluster of two or more nucleons may be in a state in either the discrete or the continuous spectrum. Assuming that the states $|j,\ m\rangle$ are mutually orthogonal and normalized,

$$\langle j,m|j',m'\rangle=\delta_{jj'}\delta_{mm'}, \tag{8}$$

we construct from them the projection operator

$$\mathscr{P}=\sum_{j,m}|j,m\rangle\langle j,m|, \tag{9}$$

which includes all states of open channels. Application of the projection operator to the wave function of the system in the form

$$\mathscr{P}\Psi=\sum_{j,m}u_j^{(m)}(r_m)\,|j,m\rangle,\quad u_j^{(m)}(r_m)=\langle jm|\Psi\rangle \tag{10}$$

leads to separation of the subspace of open-channel states. The amplitude $u_j^{(m)}(r_m)$ describes the relative motion of the two clusters of m and $A-m$ nucleons; r_m is the distance between their centers of mass.

The projection operator and its complement Q, which projects onto the subspace of closed channels, have the properties

$$\mathscr{P}^2=\mathscr{P},\quad Q=I-\mathscr{P},\quad \mathscr{P}Q=0. \tag{11}$$

Application of the projection operator to the Schrödinger equation (7) with allowance for the properties (11) leads to an equation with an effective nonlocal Hamiltonian H:[5,28]

$$\begin{aligned}&(E-H)\mathscr{P}\Psi=0,\\ &H=\mathscr{P}[\hat{H}+\hat{H}Q(E^{(+)}-Q\hat{H}Q)^{-1}Q\hat{H}]\mathscr{P},\\ &E^{(+)}=E+i\gamma,\quad \gamma\to+0.\end{aligned} \tag{12}$$

The Green's function in the Hamiltonian H is represented in terms of the energy eigenvalues ε_n, ε and eigenfunctions Φ_n, Φ_ε of the discrete and continuous spectra, respectively, of the Hamiltonian QHQ:

$$(E^{(+)}-Q\hat{H}Q)^{-1}=\sum_n\frac{\Phi_n\rangle\langle\Phi_n}{E-\varepsilon_n}+\int d\varepsilon\,\frac{\Phi_\varepsilon\rangle\langle\Phi_\varepsilon}{E^{(+)}-\varepsilon}. \tag{13}$$

If the energy varies within a certain group of N resonances, this group of singular terms must be separated from the Green's function (13); the remainder will be weak functions of the energy. After substitution of (13) in (12), the Hamiltonian H can be represented as a sum of a resonance part H_r and a potential part H_p:

$$\begin{aligned}&H=H_r+H_p,\quad H_r=\sum_{\nu=1}^{N}\frac{\mathscr{P}\hat{H}Q\Phi_\nu\rangle\langle\Phi_\nu Q\hat{H}\mathscr{P}}{E-\varepsilon_\nu},\\ &H_p=\mathscr{P}\Bigg[\hat{H}+\sum_{n\neq\nu}\frac{\hat{H}Q\Phi_n\rangle\langle\Phi_nQ\hat{H}}{E-\varepsilon_n}\\ &\qquad+\int d\varepsilon\,\frac{\hat{H}Q\Phi_\varepsilon\rangle\langle\Phi_\varepsilon Q\hat{H}}{E^{(+)}-\varepsilon}\Bigg]\mathscr{P}.\end{aligned} \tag{14}$$

In accordance with this, the solution

$$\mathscr{P}\Psi=\sum_c\left(\mathscr{T}_c-\sum_c U_{c'c}\mathscr{G}_{c'}\right),\quad U_{c'c}=U_{c'c}^{(n)}+U_{c'c}^{(r)} \tag{15}$$

of Eq. (12) in the subspace of open channels c contains potential, $U^{(p)}$, and resonance, $U^{(r)}$, parts in the collision matrix U; $\mathscr{T}_c$ and $\mathscr{G}_c$ are incoming and outgoing spherical waves.[23]

The resonance part of the collision matrix has the form[5]

$$\begin{aligned}&U_{c'c}^{(r)}=\sum_i\frac{(A_i)_{c'c}}{E-E_i},\\ &A_i=\sum_{\nu,\mu}X_\nu^i(X_\mu^i)^+V_\nu V_\mu^+,\\ &V_\nu=\langle\Phi_\nu Q\hat{H}\mathscr{P}(\mathscr{P}\Psi)_p\rangle,\end{aligned} \tag{16}$$

where X_ν^i are eigenfunctions, E_i are complex eigenvalues of the equations

$$\begin{aligned}&\sum_\nu|(E-\varepsilon_\mu)\delta_{\mu\nu}-W_{\mu\nu}|X_\nu=0,\\ &W_{\mu\nu}=\langle\Phi_\mu Q\hat{H}\mathscr{P}\frac{1}{E^{(+)}-H_p}\mathscr{P}\hat{H}Q\Phi_\nu\rangle,\\ &\sum_\nu(X_\nu^i)^+X_\nu^j=\delta_{ij},\quad \sum_i(X_\nu^i)^+X_\mu^i=\delta_{\mu\nu},\end{aligned} \tag{17}$$

and the function $(\mathscr{P}\Psi)_p$ satisfies the equation

$$(E-H_p)(\mathscr{P}\Psi)_p=0 \tag{18}$$

and also the condition of being a superposition of an incoming and outgoing wave in the region of the reaction channels.

Not every resonance term of the matrix (16) has the Breit–Wigner form with numerator proportional to the

imaginary part of the denominator. Indeed, from the sum rule for the eigenvalues of Eq. (17),

$$\sum_i E_i = \sum_\mu (\varepsilon_\mu + W_{\mu\mu}),$$

$$\sum_i \mathrm{Im}\, E_i = \sum_\mu \mathrm{Im}\, W_{\mu\mu} = -\Gamma/2, \quad \Gamma = 2\pi \sum_\mu V_\mu V_\mu^+, \tag{19}$$

$$\sum_i \mathrm{Re}\, E_i = \sum_\mu (\varepsilon_\mu + \mathrm{Re}\, W_{\mu\mu}) = \sum_\mu (\varepsilon_\mu + \Delta_\mu),$$

$$\Delta_\mu = \langle \Phi_\mu Q \hat{H} \mathscr{P} \left(P \frac{1}{E^{(+)} - H_p} \right) \mathscr{P} \hat{H} Q \Phi_\mu \rangle$$

we find that the imaginary part is not proportional to A_i (16). However, the sum $\Sigma_i A_i = \Sigma_\mu V_\mu V_\mu^+$ is proportional to the total width Γ (19) of the resonance. Therefore, the Breit–Wigner formula holds on the average. For a single resonance, the Breit–Wigner formula is valid. In Eq. (19), Δ_μ is the energy shift of the resonance, and the symbol P denotes the principal value of the integral.

The nonresonant energy dependence is determined by the solution of Eq. (18) regular at the origin. Above the threshold ($\rho^2 > 0$), this dependence can be represented explicitly in the form[23,29,30]

$$U_{c'c} = P_{c'}^{1/2} M_{c'c} P_c^{1/2}, \quad M_{c'c} = \mathfrak{M}_{c'c} + \sum_i \frac{(a_i)_{c'c}}{E - E_i},$$

$$(A_i)_{c'c} = P_{c'}^{1/2} (a_i)_{c'c} P_c^{1/2}, \quad U_{c'c}^{(p)} = P_{c'}^{1/2} \mathfrak{M}_{c'c} P_c^{1/2},$$

$$P_c = P_l = \frac{\rho^{2l+1}}{[(2l-1)!!]^2} Q_l(\eta), \tag{20}$$

$$Q_l(\eta) = C_0^2 \prod_{m=1}^{l} (1 + \eta^2/m^2) \exp(2i\omega_l),$$

$$C_0^2 = 2\pi\eta / [\exp(2\pi\eta) - 1].$$

The energy dependence of P_c near the threshold is the same as the dependence of the penetrability P_c (2) in R-matrix theory. Far from the threshold ($\rho \gg 1$), $P_c \approx$ const in an energy interval < 1 MeV.

For uncharged particles, $\eta = 0$, the function $Q_l(\eta) = 1$. The matrix elements $\mathfrak{M}$ and (a_i) are weak functions of the energy in the threshold region. They can be represented as series expansions in positive integer (beginning with zero) powers of the energy, as follows from the $\rho \to 0$ asymptotics of the solutions of a one-dimensional Schrödinger equation.[23,29] The level shift Δ_μ has a similar energy dependence. The energy dependence of the resonance-level widths Γ_c is determined in accordance with (6), in which the penetrability P_c must be replaced by the function P_c (20), and the reduced width $\gamma_{\lambda c}^2$ by the parameter γ_c^2, which is proportional to it and has energy dependence analogous to that of Δ_μ, $\mathfrak{M}$, and a_i.

The energy dependence of the collision matrix below the threshold can be obtained by analytic continuation to the complex energy plane. In the region of a two-particle neutron threshold ($\eta = 0$), it is sufficient for this to make the substitution $E - E_q \to -|E - E_q|$ and $\rho \to i|\rho|$ in the expressions (20). If two charged particles are produced in the threshold channel, the threshold point is essentially singular in the complex-energy plane. Analytic continuation to the below-threshold region is made with a wave function valid both above and below the threshold.[3,4] This problem requires additional investigations.

The unitarity of the collision matrix makes it possible to determine the energy dependence near the threshold in all open (nonthreshold) reaction channels. In the region of a neutron threshold, the matrix element of a nonthreshold channel can be expanded in powers of $\rho = kr$. Restricting ourselves to the first two terms, we find[25]

$$U_{ij} = \mathring{U}_{ij} - \frac{1}{2} \sum_k \mathring{U}_{ik} \sum_n U_{nj} U_{nk}^*, \quad k = i, j. \tag{21}$$

Here, $\mathring{U}_{ij}$ is the value of U_{ij} in the absence of a threshold. The summation over k includes all open channels. The expansion (21) is valid both above and below the neutron threshold.

We consider a threshold in which three particles are produced—one neutral and two charged ones with charges of the same sign. In this case, there is a logarithmic singularity at the threshold point.[31,32] The energy dependence of P_c (20) can be represented in the form[33]

$$P_c^{1/2} = a(E - E_q) + b(E - E_q)^2 [1 + c \ln(E - E_q)], \quad E \gtrless E_q. \tag{22}$$

Here, a, b, and c are constant complex quantities. The energies are expressed in dimensionless units.

If a three-particle threshold channel involves formation of a neutron and an unstable nucleus consisting of two particles, $Y^* \to b + c$, then[4,34]

$$P_c \propto [\mathrm{Re}(E - E_r + i\gamma/2)]^{l+1/2}, \tag{23}$$

where the threshold energy $E_q \to E_r - i\gamma$ is replaced by the energy eigenvalue of the nucleus Y^*. The imaginary part of the energy leads to a smearing of the threshold singularity by an amount of the order of the level width γ.

It is obvious that in Feshbach's unified theory there are no restrictions on the number of open channels and resonances of the compound nucleus. The energy dependence of the cross sections of nonresonance reactions near the threshold in the case $l = 0$ corresponds to the energy dependence of the cross sections (3)–(4) obtained in R-matrix theory.

The resonating-group method is a model method

A description and applications of the resonating-group method can be found in many studies. We are interested in those in which the method is applied to the description of threshold phenomena in light-nucleus reactions. The method uses a many-particle oscillator basis to expand the wave function of the system. In the basis space of functions one distinguishes several subspaces corresponding to relative motion of clusters in different channels and in bound states. The wave function of the system is constructed as a series expansion with respect to the basis states $|\nu, \alpha\rangle$ of these subspaces:[6,26]

$$\Psi=\sum_{\nu,\alpha} C_{\nu}^{\alpha}|\nu,\alpha\rangle, \tag{24}$$

where ν is the index of the basis function, and α is the set of quantum numbers that identify the cluster states in the continuous and discrete spectra.

To find the expansion coefficients of the wave function, it is necessary to solve the system of linear algebraic equations

$$\sum_{\nu',\alpha'} \langle\alpha,\nu|\hat{H}-E|\nu',\alpha'\rangle C_{\nu'}^{\alpha'}=0, \tag{25}$$

where $\hat{H}$ is the Hamiltonian of the nucleus.

If a complete oscillator basis is used in the calculations, the results must be independent of all parameters. In reality, however, one can choose only part of a complete basis, making plausible assumptions about the physics of the phenomena in the nucleon system. The influence of the part of the basis not included within the treatment must be manifested in the introduction of certain free parameters. One such parameter is the oscillator radius r_0 (or oscillator frequency $\omega=\hbar^2/\mu r_0^2$), which is chosen to give the best description of the structural features of the system. The realistic Volkov[35] and Hasegawa–Nagata[36] potentials are used as nucleon–nucleon interaction potentials.

The resonating-group method has been used to investigate the few-nucleon systems with $A=4$ (Refs. 37 and 38), $A=5$ (Refs. 39 and 40), and $A=6$, 7 (Refs. 41 and 42). Taken together, the results of these studies reveal the strength and weaknesses of the resonating-group method. The strengths include: 1) comparative simplicity (relative to multidimensional Schrödinger or Faddeev–Yakubovskiĭ equations[32]) of the solution of the system of linear algebraic equations; 2) high sensitivity of the solution to the chosen system of subspaces of functions used as an expansion basis for the wave function of the system; 3) the possibility of calculating all physical phenomena observed experimentally. A weakness of the method is the unpredictability of the results in the sense that it is difficult to predict in advance the consequence of restricting the function basis to a few subspaces of selected channels. The choice of the model of nucleon–nucleon interactions plays an important part and cannot be readily made in advance.

Analytic *S*-matrix theory

A Hamiltonian and other operators of quantum mechanics is not used in S-matrix theory.[7] It retains only the superposition principle. It is assumed that the momenta and directions of particle spin before and after a collision are the only observable quantities.

The central property of the S matrix is its analyticity as a function of the momenta of the incoming and outgoing particles. The particles are associated with poles. The most important of them are those that can be expressed in terms of channel invariants—the square S_c of the total energy in the center-of-mass system of channel c:

$$S_c=\left(\sum_{i\in c} p_i\right)^2, \tag{26}$$

where p_i is the momentum of particle i.

In addition, for each channel c there exists a threshold S_c^t equal to the square of the sum of the masses of all the particles in the channel:

$$S_c^t=\left(\sum_{i\in c} m_i\right)^2.$$

The channel thresholds are branch points and are intimately related to the unitarity of the S matrix by the $+i\varepsilon$ rule for avoiding the branch points. The analytic continuation is made on the physical sheet and is specified by describing cuts from each threshold branch point in the positive direction along the real axis of the channel-invariant variable to infinity. The rule for avoiding the branch points permits an analytic continuation of unitarity (or calculation of the discontinuity of the reaction amplitude). The unitarity relation is the basis in the formulation of dynamical models. For example the avoidance of one branch point corresponding to the threshold of a two-particle channel leads to a discontinuity in the connected four-point function:

$$M_{ba}(S)-M_{ba}(S_n)=\frac{1}{16\pi^2}\frac{q_n(S)}{\sqrt{S}}\int d\Omega_n M_{bn}(S_n)M_{na}(S),$$

where S_n lies directly below S on the sheet that can be reached by going once counterclockwise around the nth branch point; $q_n(S)$ is the modulus of the momentum of each of the two particles in channel n; Ω_n is the branch-point avoidance contour. Despite the apparent transparency of analytic S-matrix theory, its application in practical calculations encounters serious difficulties. This is due, in the first place, to the two-dimensionality of the Lorentz-invariant reaction amplitude, the independent variables of which are two of the three quantities s, t, and u, which are related by the equation

$$s+t+u=\sum_{i=4}^{4} m_i^2,$$

which is obtained from the momentum 4-vectors.

In the framework of a nonrelativistic model, the coupling constants and other dynamical characteristics can be determined. For example, in a resonance–particle system the analytic properties of the amplitude[43] there have been studies of, and of the state spectrum,[44] which exhibits an anomaly with a point of accumulation of resonances at the threshold of the masses of the resonance and the particle.

Dispersion theory of nuclear reactions

The dispersion (diagrammatic) approach uses field-theory methods to calculate the cross sections of nuclear reactions at low energies. Mandelstam's double dispersion relations[8] determine the analytic properties of the amplitude as a function of the two independent variables s and t. Augmenting the dispersion relation by the unitarity condition, it is possible to obtain a closed scheme for a dynam-

ical description of the system that is equivalent to the Schrödinger equation.[45,46]

A dispersion theory is developed in Refs. 47 and 48 for the description of the resonance structure of nuclear-reaction cross sections near two-particle thresholds. For the partial-wave amplitudes there is a system of integral relations similar to Bethe–Salpeter equations[49] for each value of the total angular momentum J. Near the threshold, this system of relations is transformed in the effective-range approximation into a system of algebraic equations whose solutions have complex poles. These poles correspond to threshold states of the compound nucleus. It was shown in Ref. 48 that the expression obtained by using a method of quantum field theory to find the amplitude in the effective-range approximation is identical to the amplitude obtained in nonrelativistic quantum mechanics.[50]

3. COMPLETE AND INCOMPLETE EXPERIMENTS. REQUIREMENTS ON THE EXPERIMENTAL DATA

An important question to answer is that of what experiments give the necessary and sufficient information for unique recovery of a wave function near a threshold. The theoretical solution of this problem not only determines the necessary set of experimental data and a method of recovering the wave function but can also help to formulate the basic requirements on an experiment and establish which problems can be solved in an incomplete experiment.

Elastic scattering of two spinless particles near a threshold for production of two neutral spinless particles and in the absence of resonances of the intermediate system was considered in Ref. 4. It was shown that a necessary and sufficient condition for recovery of the wave function in the elastic-scattering channel is measurement at each scattering angle, of the cross section at the threshold point and of its slopes to the left and to the right of the threshold. The cross section in the threshold reaction channel can be determined from these data.

We have investigated the same problem when there is a compound-nucleus resonance near a threshold. The energy dependence of the collision matrix in the threshold channel is determined by the expressions (20). In the open channel, it is determined from the unitarity relation ($E>E_q$):

$$|U_{l'l}|^2=1-\frac{\rho^{2l'+1}P_l}{[(2l'-1)!!]^2}|M_{l'l}|^2,$$
$$U_{l'l}=e^{i(\delta_l+\delta_{l'})}\left(1-\frac{1}{2}\frac{\rho^{2l'+1}P_l}{[(2l'-1)!!]^2}|M_{l'l}|^2\right), \quad (27)$$
$$\rho=k_n r\ll 1, \quad P_l\approx\text{const},$$

where δ_l is the phase shift of potential scattering, and k_n is the wave number of the relative motion in the neutron channel. Below the threshold ($E<E_q$), the wave number $\to i$ becomes $|k_n|$. The unitarity condition is satisfied up to terms of order ρ^{2l+1}. In the complete threshold region, we have the condition

$$|e^{i\delta_l}|=1, \quad E\gtrless E_q. \quad (28)$$

Therefore, the phase shift δ_l is real both above and below the threshold. Its series expansion can contain only integer powers of the energy, including negative ones:

$$\delta_l=\delta_l^{(0)}+\delta_l^{(1)}E+\ldots+\arctan\frac{\Gamma_l}{2(E_l-E)}. \quad (29)$$

The pole term is responsible for the resonance elastic scattering. In accordance with (19) and (20), $\mathfrak{M}_l$, a_l, and Δ_l are constants up to the first term of the expansion in powers of E. For scattering of spinless particles, $l=l'$. We shall calculate the energy dependence of the elastic-scattering cross section near a threshold. Without loss of generality, we can set the resonance angular momentum equal to zero, $l_0=0$. In the matrix elements (27) of U, we shall ignore the powers of ρ above the first. For angular momentum $l=0$, we find

$$U_0=e^{2i\delta_0}\left(1-\frac{1}{2}\rho|M_0|^2\right), \quad e^{2i\delta_0}$$
$$=e^{2i\delta_0^{(0)}}\left(1-\frac{i\Gamma_0}{E-E_0+i\Gamma_0/2}\right). \quad (30)$$

For $l>0$,

$$U_l=e^{2i\delta_l}, \quad \delta_l\cong\text{const}. \quad (31)$$

Substituting (30) and (31) in the expression for the differential elastic-scattering cross section,

$$\sigma(\theta,E)=|f(\theta,E)|^2,$$
$$f(\theta,E)=\frac{1}{2ik}\sum_l(2l+1)P_l(\cos\theta)(U_l-1), \quad (32)$$

we determine its energy dependence:

$$\sigma(\theta,E)=|f(\theta,E_q)|^2-|f(\theta,E_q)|\frac{\Gamma_0}{k}\mathscr{L}[\text{co}(E-E_0)+\text{si}\ \Gamma_0/2]+\frac{\mathscr{L}\Gamma_0^2}{4k^2}-|f(\theta,E_q)|\frac{|\rho||M_0|^2}{2k}$$
$$\times\begin{cases}(\text{si}-\Gamma_0\mathscr{L}[\text{co}(E-E_0)+\text{si}\ \Gamma_0/2]), & E>E_q,\\ (\text{co}+\Gamma_0\mathscr{L}[\text{si}(E-E_0)-\text{co}\ \Gamma_0/2]), & E<E_q,\end{cases} \quad (33)$$
$$\mathscr{L}=[(E-E_0)^2+\Gamma_0^2/4]^{-1},$$
$$\text{si}=\sin[2\delta_0^{(0)}-\alpha(\theta)], \quad \text{co}=\cos[2\delta_0^{(0)}-\alpha(\theta)].$$

The amplitude

$$f(\theta,E_q)=|f(\theta,E_q)|\,e^{i\alpha(\theta)} \tag{34}$$

also describes potential elastic scattering in the threshold region with accuracy $\sim\rho^2$ and does not depend on the energy. To the same accuracy, the phase shifts $\delta_0^{(0)}$ and $\alpha=\alpha(\theta)$ are constants. Comparison of the cross section (33) with the nonresonance cross section of Ref. 4 shows that in the absence of a resonance amplitude they are identical. The same can be said of the threshold cross section

$$\sigma_n=\frac{\pi}{k^2}\sum_l(2l+1)|U_l^{(n)}|^2\cong\frac{\pi}{k^2}|\rho||M_0|^2. \tag{35}$$

The cross section (33) can be generalized to the case of several resonances near a reaction threshold by using the expressions (15) and (16) for the matrix U. Such a generalization does not introduce significant changes into the energy dependence of the cross section. Therefore, we shall solve the problem of a complete experiment for the case of one resonance, avoiding unnecessary complications.

A compound-nucleus resonance introduces four additional parameters into the description of the cross section—the complex quantity a_0 and the two real quantities E_0 and Γ_0. Since the amplitude of the threshold channel occurs quadratically in the cross section (33), the phase of the amplitude of potential interaction does not come into consideration. Five constant parameters remain. Besides them, the cross section (33) contains all the quantities $f(\theta, E_q)$ and $\alpha(\theta)$, which depend on the angles, and $\alpha(\theta)$ occurs in the combination $2\delta_0^{(0)}-\alpha$ with the constant $\delta_0^{(0)}$. For given scattering angle θ_0, determination of the seven parameters

$$|\mathfrak{M}_0|,\ \mathrm{Re}\ a_0,\ \mathrm{Im}\ a_0,\ E_0,\ \Gamma_0,\ |f(\theta_0,E_q)|,$$
$$\times[2\delta_0^{(0)}-\alpha(\theta_0)] \tag{36}$$

is possible if the excitation function $\sigma(\theta_0, E)$ is measured at not less than seven energy points in the region to the left and to the right of the threshold. The parameters are found by variation in accordance with the least-squares method. The angular dependence of the parameters $f(\theta, E_q)$ and $2\delta_0^{(0)}-\alpha(\theta)$ is determined from the theoretical least-squares description of the squares of the excitation functions $\sigma(\theta, E)$ measured at various angles. As a result of this, we obtain a series expansion in Legendre polynomials $P_l(\cos\theta)$, of

$$e^{-i(2\delta_0^{(0)}-\alpha(\theta))}|f(\theta,E_q)|=e^{-2i\delta_0^{(0)}}f(\theta,E_q). \tag{37}$$

From the expansion of the amplitude (32) in Legendre polynomials at $E=E_q$ all $U_l=e^{2i\delta_l}$ for $l>0$ and $U_0=e^{2i\delta_0^{(0)}}$ can be determined. Thus, near the reaction channel the phase-shift analysis can be made uniquely. In addition, the reaction cross section (35) can be determined, since the first five parameters (36) are known from the phase-shift analysis. We summarize the results. A complete experiment for phase-shift analysis of elastic scattering near the reaction threshold is provided by measurement of the excitation function below and above the reaction threshold at a number of energy points equal to or greater than the number of parameters (36). The excitation functions must be measured at different angles in order to obtain a true expansion of the scattering amplitude in Legendre polynomials. This result is valid for scattering of spinless particles in the region of a two-particle threshold with production of a neutral particle. In the case of scattering of particles with spin, a complete experiment will also include measurements of the analyzing power (spin–orbit and spin–spin correlations) with a view to determining the expansion of the scattering amplitude with respect to functions of the total angular momentum of the system. Otherwise, the principle for recovering the scattering amplitude is analogous to the case of spinless particles.

We shall analyze in somewhat more detail the most typical examples of an incomplete experiment and establish what information about the nuclear system can be obtained from them.

A. Measurement of the excitation function at one angle θ

In this case, all the parameters (36) can be determined. By means of them, we find (37) at the energy threshold point E_q and at angle $\theta=\theta_0$, and also the energy of the compound-nucleus resonance and its total and partial widths in accordance with the expressions

$$\rho|a_0|^2=\Gamma_n\Gamma_0,\quad 2\rho\gamma_n^2=\Gamma_n,\quad \Gamma=\Gamma_0+\Gamma_n, \tag{38}$$

where γ_n^2 is the reduced partial (neutron) width. Simultaneously, the reduced potential amplitude $|\mathfrak{M}_0|$ for transition to the threshold channel is determined.

B. Measurement of the integrated excitation function

In this case, one measures the cross section

$$\sigma(E)=\frac{\pi}{k^2}\sum_l(2l+1)|U_l-1|^2, \tag{39}$$

We substitute in (39) the elements (30) and (31) of the S matrix:

$$\sigma(E)=\sigma(E_q)+\pi\mathscr{L}\frac{\Gamma_0^2}{k^2}\left(1-2\frac{(E-E_0)}{\Gamma_0}\sin 2\delta_0^{(0)}+2\sin^2\delta_0^{(0)}\right)-\sigma_n(k_n)$$
$$\times\begin{cases}(2\sin^2\delta_0^{(0)}-\mathscr{L}[\Gamma_0(E-E_0)\sin 2\delta_0^{(0)}+\Gamma_0^2(1+\sin^2\delta_0^{(0)})]), & E>E_q,\\ (\sin 2\delta_0^{(0)}+\mathscr{L}[2\Gamma_0(E-E_0)(1+\sin^2\delta_0^{(0)})-\sin 2\delta_0^{(0)}\Gamma_0^2/2]), & E<E_q.\end{cases} \tag{40}$$

The description of the integrated excitation function by the theoretical energy-dependent function (40) by the least-squares method permits determination of the parameters

$$\sigma(E_q),\sigma_n(k_n),E_0,\Gamma_0,\delta_0^{(0)}.$$

Thus, from analysis of the integrated excitation function it is possible to find the cross section for elastic potential and resonance scattering and the interference of them, the parameters of the compound-nucleus resonance, and the phase shift of the potential scattering at the point of the reaction threshold. If the amplitude of potential interaction is ignored in comparison with the amplitude of resonance interaction in the amplitude M_0 of the threshold reaction, then the reduced neutron width can be estimated from the expressions (40). In connection with the problem of complete and incomplete experiments, the requirements on the experimental data can be found. Naturally, limits must be set on the energy resolution and the experimental errors. We estimate these limits as follows. We calculate first of all the number of independent real parameters in the theoretical function of the energy by means of which the experimental excitation functions are analyzed. Each element of the collision matrix of the resonance type (28) has six parameters, while each element of nonresonance type has only two. Having estimated by means of the reaction energetics and the angular momenta what matrix elements (and in which channels) play the important parts, we can count the number of parameters. All the remaining matrix elements can be approximated by a constant or by some simple function of the energy. However, the number of parameters must not exceed 50–60. This upper limit is determined by the technical capabilities of computers currently accessible to us. Least-squares minimization of a functional with a larger number of parameters is ineffective. To determine 50–60 parameters by the least-squares method, the number of experimental points must be of order 100. The near-threshold energy interval can be estimated from the condition $\rho=kr<1$ and is equal to 1 MeV for light nuclei. As a result, from these two numbers we obtain the required energy resolution:

$$\Delta E\approx 10 \text{ keV}. \tag{41}$$

Besides the estimate (41), which is obtained independently of the structure of the excitation function in the threshold region, another estimate due to this structure may also exist. The threshold singularities ("cusps," "steps") extend in energy over about 100 keV. Therefore, the energy resolution (41) is sufficient to describe the threshold singularity. Compound-nucleus resonances can have widths in the range of energies from a few electron volts to several mega-electron-volts. An energy resolution a few times less than the resonance width is needed for their experimental description. The most typical values of the widths of resonances in the region of light nuclei are above several tens of kilo-electron-volts. For their description, the energy resolution (41) is also sufficient.

We consider the requirements imposed on the accuracy of the experimental data. The requirements depend not only on the number of parameters in the theoretical function of the energy but also on its form. We estimate the accuracy for a power-law function of the energy—the weakest energy dependence. We take the difference of a function of the energy of the minimum power 1/2 and a constant in the threshold region $\rho=kr<1$ and impose the condition that in the greater part of this region the difference be greater than twice the experimental errors in the function $\rho\sim(E-E_q)^{1/2}$. Setting the constant equal to zero, we find

$$\rho>2\sigma, \quad 0.1<|E-E_q|<0.5.$$

The region in which the function of the energy can differ from a constant is defined nominally by the interval [0.1, 0.5]. From this there follows the dependence of the possible growth of the experimental errors with increasing distance from the threshold:

$$\sigma<(0.05-0.1). \tag{42}$$

Thus, the experimental errors must not exceed a few percent.

4. PROBLEMS OF MULTIPARAMETER DESCRIPTION OF EXPERIMENTAL DATA NEAR A THRESHOLD

An element

$$U_{c'c}=P_{c'}^{1/2}M_{c'c}P_c^{1/2}, \quad M_{c'c}=\mathfrak{M}_{c'c}+\frac{(a_i)_{c'c}}{E-E_i}$$

of the collision matrix contains three unknown complex quantities: $\mathfrak{M},(a_i)$, which must be found by analysis of experimental data in the region of the threshold. Usually, all three quantities are constant near a threshold. There may be an exception in the case of the imaginary part of E_i, which is proportional to the total width of the resonance, if just one channel (19) is open:

$$\text{Im } E_i=\frac{\Gamma_i}{2}\sim(E-E_q)^{l+1/2}.$$

Although the real part of E_i does depend on the energy, its principal term is a constant:[23]

$$\text{Re } E_i=\Delta_i=\Delta_i^{(0)}+\Delta_0^{(1)}E+\dots .$$

There is a similar energy dependence for $\mathfrak{M}$ and (a_i). Thus, the minimum number of parameters in an element of the collision matrix is two for the potential term and four for each resonance term. In the case of resonance scattering when only the elastic scattering channel is open,[5]

$$A_i=\frac{-1}{\pi}\text{Im } E_i \exp(2i\delta),$$

the number of parameters in an element $U_{c'c}$ can be reduced from six to three.

This counting of the parameters shows that a wave function containing up to about ten elements of the collision matrix can be analyzed by the least-squares method. A greater number of states can usually be included in the case of a small number of resonance states of the compound nucleus or if certain terms in the expansion with respect to the energy are ignored. As a rule, the principal term of the expansion is retained. Terms of higher order are retained if necessary for physical reasons (for example, there is retention of terms with orbital angular momenta $l>1$ in the threshold channel) and when the experimental errors do not exceed 2–3%. If the experimental errors are 5–10%, there is no point in retaining terms in the expansion with respect to the energy apart from the leading term, since the varied parameters are correlated. Correlated parameters can vary in wide ranges without a change in the value of χ^2. For successful least-squares analysis it is sometimes helpful to eliminate from variation some strongly correlated parameters, fixing their values at certain physically sensible constant values.

5. RESULTS OF ANALYSIS OF EXPERIMENTAL DATA

The experimentally observed threshold anomalies have been described theoretically in studies of the authors (Refs. 11–13, 25, 52, and 53) and others (Refs. 37–42, 47, and 48). We begin our presentation of the results of the theoretical analysis with our studies, in which, it seems to us, the properties of nuclear threshold states have been most systematically investigated. Several highly excited ^{10}Be states at energies from 17 to 23 MeV were analyzed. The states were investigated in the ^{7}Li(t, p)^{9}Li, ^{7}Li(t, α_0), ^{7}Li(t, α_1), and ^{7}Li(t, n) reactions[52,57] with energy resolution 20 keV and the rather low error 2–3%. In the process, we shall analyze the ^{7}Li(^{3}He, p)^{9}Be reaction,[14] with formation of the compound nucleus ^{10}B, which is a member of the same isobaric multiplet with $A=10$. We shall then present the results of phase-shift analysis of proton elastic scattering by ^{7}Li at energies $E_p=1.5$–3 MeV in the region of two neutron thresholds of the ^{7}Li(p, n)^{7}Be reaction. At the end of the section, we shall describe the results of analyses made by other authors.

Analysis of threshold anomalies in the excitation function of the ^{7}Li(t, p)^{9}Be reaction

The results of measurement of the integrated excitation functions for the ^{7}Li(t, p)^{9}Li, ^{7}Li(t, α), ^{7}Li(t, d), and ^{7}Li(t, n) reactions at energies $E_t=3$–10 MeV of the incident tritons in the laboratory system are presented in Refs. 53–56. Around the energies $E_t=5.649$ and 8.339 MeV, at which the channels of the ^{7}Li(t, n)^{9}Be($T=3/2$) reaction are opened,[10] giant anomalies (up to 30%) are observed in the ^{7}Li(t, p)^{9}Li excitation function. To explain the shape and intensity of the anomalies, it was necessary to assume that the threshold neutrons are formed in a state with orbital angular momentum $l_n=0$ and that near the thresholds there are ^{10}Be states with probable isospin $T=2$, which are analogs of the ground and excited states of ^{10}Li. In Ref. 55, an analysis of the shape of the neutron yield curve near the first threshold as a function of E_t showed that $l_n=0$. In addition, a shell-model analysis of the structure of light-nucleus levels made in Ref. 58 showed that the ground state of the ^{10}Li nucleus has the configuration $(1s)^4(1p)^5(2s1d)^1$ and spin–parity $J^\pi=2^-$, which corresponds to $l_n=0$. Subsequently, in Refs. 11–13, it was conjectured that the second anomaly has the same nature as the first. Both of these states represent the ^{9}Be nucleus in the first and the second excited states with $T=3/2$ together with a weakly bound neutron. This is supported by the results of Ref. 58, from which it follows that the second excited ^{10}Be state with $T=2$ has spin–parity $J^\pi=1^-$. The threshold neutron must be emitted with $l_n=0$.

A theoretical analysis of the two threshold anomalies was made on the basis of the above approach in Refs. 11–13. The theoretical function of the energy (integrated cross section) was constructed from the matrix elements (20) and (21) with sets of quantum numbers that included the orbital angular momenta of the triton, proton, and threshold neutron:

$$l_t,l_p=0,1,2, \quad l_n=0,1. \tag{43}$$

With allowance for the spins and parities of the incident and emitted particles in the p and n channels,

$$s_p=s_t=1^+/2, \quad s_{\mathrm{Li}}=s_{\mathrm{Be}}=3^-/2,$$

we find the values of the total angular momentum and parity of the system: $\mathbf{J}=\mathbf{l}+\mathbf{s}$, where $\mathbf{s}$ is the spin of the channel.

To reduce the number of parameters in the theoretical function, all orbital angular momenta except zero were ignored in the first approximation. A second simplification was to make the analysis in the single-channel approximation. For this, there is a strong experimental justification, namely, the absence of an energy dependence (except for the Coulomb dependence) in the excitation functions for all channels except the (t, p) reaction channel and the experimentally uninvestigated elastic-scattering channel. The end effect of the second assumption was that the matrix elements for all reaction channels except the (t, p) reaction were set equal to a constant multiplied by the penetrability factors C_0^2 (20) in the entrance and exit channels. As a result, the integrated reaction cross section depends on the energy as follows:[11–13]

$$\sigma_{tp}=\frac{C_t^2C_p^2}{E}\left\{A+B_\tau|E-E_q|^{1/2}+(1-C_\tau|E-E_q|^{1/2})\times\frac{D_0+D_1E}{(E-E^{J\pi})^2+(\Gamma^{J\pi}/2)^2}\right\}, \quad \tau=>;<, \tag{44}$$

where the symbols $>$ and $<$ denote the regions of energies above and below the threshold E_q; $E^{J\pi}$ and $\Gamma^{J\pi}$ are the energy and width of the level of the ^{10}Be compound nucleus with isospin $T=2$. The real parameters A, B, C are

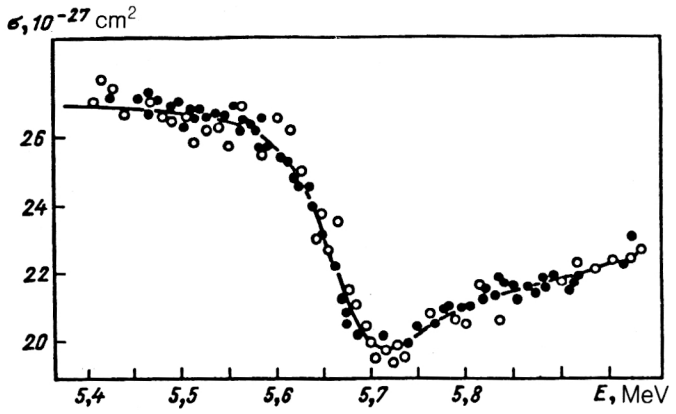

FIG. 1. Theoretical description of excitation functions of the ^{7}Li(t, p)^{9}Li reaction near the first threshold of the reaction ^{7}Li(t, n)^{9}Be* (E_x=14.3922 MeV, T=3/2).

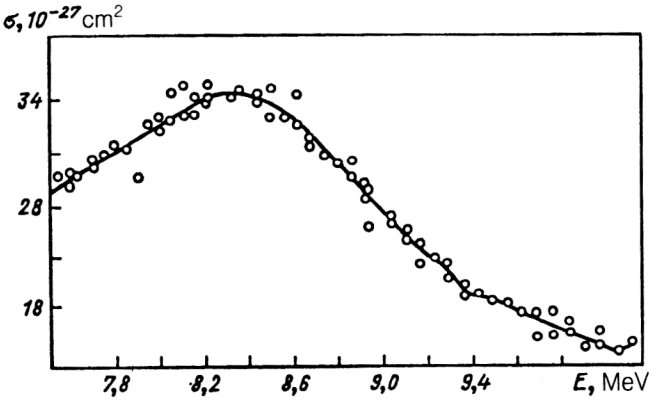

FIG. 2. Theoretical description of excitation functions of the ^{7}Li(t, p)^{9}Li reaction near the second threshold of the reaction ^{7}Li(t, n)^{9}Be* (E_x=16.975 MeV, T=3/2).

linear combinations of the squares of the amplitudes for the different quantum states of the system. The parameters D are related to the resonance-scattering amplitude by

$$D_0=\kappa(2J+1)\sum_{t,p}|\mathfrak{M}_{tp}^{J\pi}|^2 h(A_{tp}^{J\pi}),$$

$$D_1=\kappa(2J+1)\sum_{t,p}|\mathfrak{M}_{tp}^{J\pi}|^2 2\ \mathrm{Re}\ A_{tp}^{J\pi},$$

$$\kappa=\frac{\pi\hbar^2}{2\mu_t}\frac{1}{8}, \tag{45}$$

$$h(A_{tp}^{J\pi})=|A_{tp}^{J\pi}|^2-2\ \mathrm{Re}\ A_{tp}^{J\pi}E^{J\pi}+2\ \mathrm{Im}\ A_{tp}^{J\pi}\Gamma^{J\pi}/2,$$

where μ_t is the reduced mass in the entrance channel, and 1/8 is a statistical factor. The indices t and p label not only the channels but also the complete sets of quantum numbers in them. The summations indicate that it is necessary to take the sum over all orbital and final spin angular momenta of the particles.

The ^{7}Li(t, p)^{9}Li excitation function in the two threshold regions was analyzed by means of the theoretical function (44) by least-squares variation of the parameters to achieve the best description of the experimental data. The quality of the description can be judged in Figs. 1 and 2. The parameters of the theory and the physical quantities were estimated from the values found for the parameters. Table II gives data on the T=3/2 levels of the ^{9}Be nucleus and the corresponding neutron thresholds in the energy scale of the ^{10}Be compound nucleus,[10] and also the energy and widths of the T=2 levels of the Be nucleus determined from the least-squares analysis.

The reduced partial widths, in mega-electron-volts, were estimated from the relations (45):[11]

$$\gamma_p^2\cong 0.008,\quad \gamma_t^2\cong 0.128,\quad \gamma_n^2\cong 0.376.$$

It follows from this that the neutron width has the order of the single-particle width.

States with T=2 for the A=10 isobaric multiplet were also found experimentally for the ^{10}B nucleus in the excitation function of the ^{7}Li(^{3}He, p)^{9}Be reaction near two thresholds of the reaction ^{7}Li(^{3}He, n)^{9}B(T=3/2).[14] The theoretical analysis used the function of the energy (44), in which the Coulomb factor C_t^2 is replaced by C_{He}^2, the penetrability of the Coulomb barrier for ^{3}He. This approach to the analysis is justified by the equivalence of the (t, p) and (^{3}He, p) reactions apart from the Coulomb interaction and the t and ^{3}He mass difference. In these reactions, all the quantum numbers are the same. The assumptions and calculations in accordance with the shell model,[58] which are valid for ^{10}Be with T=2, are also apparently valid for ^{10}B (T=2).

The least-squares analysis of the ^{7}Li(^{3}He, p)^{9}Be excitation function gave results for the two ^{10}B levels with T=2 matching those for ^{10}Be. To see this, it is necessary to compare the data of Tables II and III.

The parameters of the ^{10}B (T=2) levels are determined with large errors due to the insufficient accuracy of the experimental data (3–6%) and small number of experimental points (about 20 points near each neutron threshold). The remaining parameters are determined with errors exceeding the values of the parameters. For this reason, it was not possible to estimate the ^{10}B partial decay widths.

The good description of the two threshold anomalies with allowance for resonance enhancement in the ^{7}Li(t, p)^{9}Li excitation function confirms the conjectured existence in ^{10}Be of two states with T=2 and $\pi=-1$ that are analogs of the ground and excited [E_x(^{10}Li)=1.8 MeV] states of ^{10}Li. Shell-model calculations[58] give for these ^{10}Li levels $J^\pi=2^-$ and 1^-, respectively. The total width of the second state is greater than that of the first by a factor of 7.5. This is mainly due to the sharp increase in the contribution of the neutron width from the first $n+^9$Be threshold channel (T=3/2, E_x=14.393 MeV). This analysis did not take into account the influence of three $n+^9$Be(T=1/2) neutron thresholds[10] on the form of the excitation function in the region of the second anomaly. The decay of the $J^\pi=1^-$, T=2 state to these levels is strongly suppressed because $l_n>0$. The influence of these three thresholds will be considered later.

TABLE II. Data on levels of the nuclei ^{9}Be ($T=3/2$) and ^{10}Be ($T=2$) near thresholds of the ^{7}Li(t, n)^{9}Be($T=3/2$) reaction.

Threshold	Energy $E^{J\pi}$ of ^{9}Be level, MeV	Threshold energies E_φ, MeV	Energy $E^{J\pi}$ of ^{10}Be level, MeV	Total widths $\Gamma^{J\pi}$, MeV
1	14,393 $J^\pi = 3/2^-$	21,205	21,218 ± 0,005 $J^\pi = 2^-$	0,112 ± 0,022
2	16,976 $J^\pi = 1/2^-$	23,788	23,034 ± 0,011 $J^\pi = 1^-$	0,84 ± 0,06

The parameters of the ^{10}Be and ^{10}B nuclei with $T=2$ determined in the analysis allow us to make some predictions concerning the properties of the $A=10$ isobaric multiplet under the assumption that they are structurally similar. It appears that the first two levels have the following structure: a core of nine nucleons ($J^\pi=3/2^-$ for the first level and $J^\pi=1/2^-$ for the second level) with $T=3/2$ and a closed $(1s)^4(1p)^5$ shell plus an outer nucleon (weakly bound or unbound with $l=0$) in the $(2s\ 1d)$ shell. The energy interval between these levels is 1.7–2 MeV. The energy of the first $T=2$ level in ^{10}C is estimated to be 23 MeV, and that of the second to be 25 MeV. The ^{10}Li and ^{10}N nuclei are mirror nuclei. It can therefore be assumed that their ground states are characterized by quantum numbers $J^\pi=2^-$ and $T=2$, and the first excited states by $J^\pi=1^-$ and $T=2$. The neutron binding energy in ^{10}Li must be close to the proton binding energy in ^{10}N.

We calculate the neutron binding energy in ^{10}Li by using the energy relations of the neighboring nucleus ^{10}Be in accordance with the formula[59]

$$\varepsilon_n(^{10}\mathrm{Li}) = \Delta E_c(^{10}\mathrm{Li}-^{10}\mathrm{Be}) - E_x(^{10}\mathrm{Be}(T=2)) + S_p(^{10}\mathrm{Be}), \quad (46)$$

where ΔE_c is the energy of the Coulomb rearrangement, determined in accordance with

$$\Delta E_c = \alpha\left(Z+\frac{1}{2}\right)/A^{1/3}+\beta,$$

$$E_x[^{10}\mathrm{Be}(T=2)] = 21.218 \text{ MeV},$$

$$S_p(^{10}\mathrm{Be}) = 10.636 \text{ MeV},$$

where S_p is the proton separation energy in ^{10}Be.[10] The Coulomb rearrangement energy was estimated in two ways—by extrapolation to $A=10$, $Z=3$ and to $A=9$, $Z=3$. The scheme using even A gives $\Delta E_c=1.342$ MeV, and for odd A we have $\Delta E_c=1.539$ MeV. The difference between them is a pairing effect.[59] The odd-A estimate of ΔE_c is sensible if it is borne in mind that ^{10}Li and ^{10}Be ($T=2$) probably have a structure of the core type [^{9}Li and ^{9}Be*($T=3/2$)] plus a neutron with binding energy near zero. The value obtained for ΔE_c corresponds to binding energies[11]

$$\varepsilon_n = -(0.03;0.23) \text{ MeV}. \quad (47)$$

The estimate[47] of the binding energy ε_n was recently confirmed experimentally[60] in the stopped-meson reaction

$$^{11}\mathrm{B}+\pi^- \rightarrow {}^{10}\mathrm{Li}+p. \quad (48)$$

Near the upper limit of the proton spectrum there was found to be a powerful resonance corresponding to production of ^{10}Li in the ground state (Fig. 3). The ^{10}Li binding energy was estimated at $\varepsilon_n=-0.15\pm0.15$ MeV. An earlier estimate[61] of the ^{10}Li binding energy from the ^{9}Be(^{9}Be, ^{8}B)^{10}Li reaction was $\varepsilon_n=-0.8$ MeV. It is obvious that these data contradict our results and the experimental data of Ref. 60.

With regard to the first excited ^{10}Li level, it is assumed in Ref. 60 that its energy is $\approx$0.5 MeV and that it cannot be resolved on the background of the powerful resonance corresponding to the ground state of the ^{10}Li nucleus, since the experimental energy resolution is 0.4 MeV. According to our assumptions, its energy is approximately 2 MeV. In the proton spectrum at this energy a bump was observed in Ref. 60, which, given sufficient statistics, could be a resonance describing the first excited level of ^{10}Li.

The excitation function of the ^{7}Li(t, p)^{9}Li reaction was analyzed above in a simplified form. No allowance was made for: 1) the Coulomb interaction of the nuclei in the

TABLE III. Data on levels of the nuclei ^{9}B($T=3/2$) and ^{10}B($T=2$) near thresholds of the ^{7}Li(^{3}He, n)^{9}B($T=3/2$) reaction.

Threshold	Energy $E^{J\pi}$ of ^{9}Be level, MeV	Threshold energies E_φ, MeV	Energy $E^{J\pi}$ of ^{10}Be level, MeV	Total widths $\Gamma^{J\pi}$, MeV
1	14,66 $J^\pi = 3/2^-$	23,095	22,7 ± 0,35 $J^\pi = 2^-$	1,1 ± 1
2	17,076 $J^\pi = 1/2^-$	25,511	24,4 $J^\pi = 1^-$	2,3

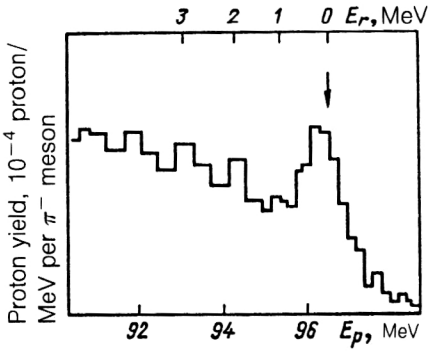

FIG. 3. Probability of production of ^{10}Li in the $\pi^- + {}^{11}\mathrm{B} \to p + {}^{10}\mathrm{Li}$ reaction.

entrance channel of the $^7\mathrm{Li}(t, n)^9\mathrm{Be}(T=3/2)$ threshold reaction; 2) threshold states with $l>0$; 3) the multichannel nature of the $^7\mathrm{Li}+t$; 4) the three neutron thresholds of the $^7\mathrm{Li}(t, n)^9\mathrm{Be}(T=1/2)$ reaction near the second $^{10}\mathrm{Be}(T=2)$ resonance; 5) the smearing of the neutron thresholds due to the finite width of the ^{9}Be* levels. A repeat analysis[62] eliminated these shortcomings in order to determine more accurately the spectroscopic characteristics of the compound-nucleus resonances and to estimate the influence on them of the changes made in the analysis. The number of partial waves included in the entrance channel was restricted to three: $l=0$, 1, 2. Even and odd waves excite negative- and positive-parity states of the Be compound nucleus, respectively:

$$J^\pi = (0,1,2,3,4)^-, \quad l_t = 0,2,$$

$$J^\pi = (0,1,2,3,)^+, \quad l_t = 1.$$

In the neutron threshold channels, it is sufficient to take into account two partial waves with l_n equal to 0 or 1. In the nonthreshold neutron and α channels the penetrability does not depend on l. In the deuteron channel, waves with $l_d \leqslant 2$ were included in the calculation. The $^7\mathrm{Li}(t, p_1)^9\mathrm{Li}$* reaction was not considered because its cross section is small [$<10\%$ of the (t, p_0) reaction[54,56]]. The number of neutron threshold channels in the considered intervals of energies E_t (5–6.3 and 8.5–10 MeV) is determined by the number of ^{9}Be states (Table IV).[10]

In the region of the first and second $n+{}^9\mathrm{Be}(T=3/2)$ neutron thresholds resonance states of $^{10}\mathrm{Be}(2^-, 2)$ and $^{10}\mathrm{Be}(1^-, 2)$ are excited, respectively. Four forms of least-squares calculations were made. Version I(10) (10 is the number of parameters) corresponds to the numerical analysis made in Refs. 11–13. A difference of the calculations in Refs. 11–13 is that the Coulomb interaction in the entrance channel is taken into account in the $^7\mathrm{Li}(t, n)^9\mathrm{Be}(T=3/2)$ threshold reaction. In version II(12) terms with $l_n=1$ are also taken into account. Calculations in version III(15) were made in the region of the first threshold with allowance for all reaction channels. In version IV(19), in the single-channel approximation, the effect of three "additional" neutron thresholds of the $^7\mathrm{Li}(t, n)^9\mathrm{Be}(T=1/2)$ reaction on the parameters of the $^{10}\mathrm{Be}(J^\pi=1^-, T=2)$ resonance state in the region of the second threshold was investigated. It can be seen from Table IV that in the region of the first threshold too there is an "additional" ^{9}Be level with $E_x=14.4$ MeV and $\Gamma=0.8$ MeV. Its influence on the resonance parameters of the $^{10}\mathrm{Be}(J^\pi=2^-, T=2)$ level can be ignored because $\Gamma \gg \Gamma^2$.

The dependence of the parameters of the $^{10}\mathrm{Be}(T=2)$ resonances on the version used is shown in Table V, which also gives the values of χ^2 for comparison of the quality of the description. The numbers of experimental points in the region of the first and second thresholds are 135 and 82, respectively.[62] The final column gives the values of $E_x^{J^\pi}$ and $\Gamma_{\mathrm{cms}}^{J^\pi}$ obtained by conversion, to the scale of the ^{10}Be nucleus of the versions II(12) for the 2^- level and IV(19) for the 1^- level.

Comparing the parameters in Table V obtained for the $^{10}\mathrm{Be}(T=2)$ levels in the various versions of the analysis[62] with the results of the calculations in Refs. 11–13 we find that the values of all the parameters apart from Γ^{1^-} agree with the corresponding parameters of Refs. 11–13, within their errors. The parameter Γ^{1^-} differs by almost a factor of two from the analogous parameter in Refs. 11–13 and is far outside the error limits. Therefore, in determining the parameters of the compound-nucleus levels it is necessary to take into account all the low-lying neutron thresholds. Decay of the $^{10}\mathrm{Be}(2^-, 2)$ state to the neutron threshold channel $n+{}^9\mathrm{Be}(3/2^-, 3/2)$ does not destroy its isospin purity. The same applies to the $n+{}^9\mathrm{Be}(1/2^-, 3/2)$ decay of the $^{10}\mathrm{Be}(1^-, 2)$ state. However, the second branch $n+{}^9\mathrm{Be}(5/2^+, 1/2)$ of the $^{10}\mathrm{Be}(1^-, 2)$ decay introduces a 12% admixture with isospin $T=1$. The analysis is incomplete. As was noted at the beginning of the section, there has been no experimental investigation of the $^7\mathrm{Li}+t$ elastic-scattering channel in the region of the two studied

TABLE IV. Levels of the nucleus ^{9}Be in the intervals $E_x=14$–15 and 16.5–17.5 MeV.

E_x, MeV	J^π	T	Γ_{cms}, keV	$(E_t)_{\mathrm{lab}}$, MeV
14,3922	$3/2^-$	3/2	0,381 ± 0,033	5,649
14,4 ± 0,3			~800	5,66
16,67 ± 0,008	$(5/2^+)$	(1/2)	41 ± 4	8,904
16,9752	$1/2^-$	3/2	0,49 ± 0,05	9,339
17,298 ± 0,007	$(5/2^-)$	(1/2)	200	9,8
17,493 ± 0,007	$(7/2^+)$	(1/2)	47	10,079

TABLE V. Parameters of levels of the nucleus ^{10}Be ($T=2$) for various versions of analysis of the ^{7}Li(t, p)^{9}Li reaction cross section.

Threshold	Parameter	Data of Refs. 11–13	I(10)	II(12)	III(15)	IV(19)	E_x, Γ_{cms}
1	E^{2^-}, МэВ	5,669	5,773	5,666±0,033	5,673	—	21,216±0,023
	Γ^{2^-}, кэВ	160	290	115±44	133	—	80±30
	χ^2		1701	1368	1363	—	—
2	E^{1^-}, МэВ	8,263	8,695	8,447	—	8,5±0,3	23,163±0,205
	Γ^{1^-}, кэВ	1200	1668	1444	—	685±570	480±400
	χ^2		1113	1088	—	1048	—

Note: The energies are given in the laboratory system, except for the ^{10}Be levels.

thresholds. If a strong energy dependence of the excitation function is found in this channel, the results of the analysis may be changed. In addition, in the ^{7}Li(t, p)^{9}Li excitation function at $E_t=5.58$ MeV a break is observed (see Fig. 1). There are two possible reasons for it: the existence of an unknown $n+^9$Be neutron threshold or overlapping of two resonance levels of the ^{10}Be compound nucleus. Both factors could be operative. We shall discuss the influence of the first. The existence of an unknown ^{9}Be level with excitation energy $E_x=14.34$ MeV is improbable, since the ^{9}Be levels have been studied in many different reactions[10] up to excitation energy 25 MeV. However, if its existence is allowed, then from the "smearing" width of the threshold singularity it may be concluded that the width of this level is $\Gamma=30$–50 keV. Therefore, the level must have isospin $T=1/2$.

A second possibility is the existence of two overlapping resonances of the ^{10}Be compound nucleus near the first neutron threshold with $T=2$. The isospins of these resonances are probably 1 and 2, since it is unlikely that both resonances have $T=2$. Being in this last case analogs of the ^{10}Li levels, the presence of spins would indicate the existence of an excited ^{10}Li state at $E_x=10$ keV. The spins of these ^{10}Be levels could be different, with opposite parities. For a near-threshold resonance the parameters will evidently be as before: $J^\pi=2^-$, $E_{t\text{lab}}=5.65$ MeV, $\Gamma_{\text{lab}}=160$ keV. The presumed parameters of the neighboring resonance are $E_{t\text{lab}}=5.56$ MeV, $\Gamma_{\text{lab}}=30$ keV (see Fig. 1).

Levels of the ^{10}Be nucleus near the threshold of the ^{7}Li+t channel

The differential reaction cross sections measured at 90° in the energy range $E_t=80$–500 keV were analyzed to establish the structure of the ^{10}Be compound-nucleus levels near the threshold of the ^{7}Li+t channel.[25] Orbital angular momenta $l>1$ can be ignored. Taking into account the spins and parities of the ground states of the ^{7}Li($3/2^-$) and $T(1/2)$ nuclei,[10] we can determine the ^{10}Be states excited in the threshold channel:

$$J^\pi=2^-,1^-,0^+,1^+,2^+,3^+. \tag{49}$$

To the α_0+^6He(0^+) reaction channels there decay four states of the ^{10}Be compound nucleus:

$$J^\pi=1^-(s=1),0^+(s=1),2^+(s=1,2), \tag{50}$$

where s is the spin of the ^{7}Li+t channel. To the α_1+^6He*(2^+) reaction channels there already decay 13, and to the neutron channels more than 20, ^{10}Be states for all pairs of the numbers J^π (49). An analysis was made of the differential S factor, defined by analogy with the astrophysical S factor:

$$S(90°,E)=\frac{d\sigma}{d\Omega}E(e^{2\pi\eta}-1)=\sum_{L=0}^{2}B_L P_L(\cos 90°)$$
$$=B_0-\frac{1}{2}B_2\,. \tag{51}$$

Here, B_2 contains not only the squares of the matrix elements but also interference terms of positive-parity states. In the (t, α_0) reaction, the 0^+ and 2^+ ($S=1$) states interfere.

The energy dependence of the S factor (51) is determined by the penetrabilities in the entrance channel and by the resonance states of the compound nucleus. The energy dependence in the exit channels of the reactions can be ignored, since the reaction energy is $Q\sim 10$ MeV:[10]

$$S(90°,E)=\sum_{J^-}p^{J^-}|M^{J^-}_{\alpha,t}|^2+(kR)^2(1+\eta^2)$$
$$\times\left\{\sum_{J^+}\left[p^{J^+}|M^{J^+}_{\alpha,t}|^2\right.\right.$$
$$\left.\left.+\sum_{J^+}q^{JJ'}\mathrm{Re}\ ((M^{J^+}_{\alpha,t})^*M^{J'^+}_{\alpha,t})\right]\right\}. \tag{52}$$

Here, p and q are known constant coefficients. The terms of opposite parity have different energy dependences.

Analysis of the S factor (52) of the ^{7}Li(t, α_0)^{6}He reaction showed that a $2^+(s=2)$ resonance state is not present in the ^{10}Be nucleus and that the parameters of the $2^+(s=1)$ resonance are close to the experimental values of Ref. 10 (Table VI). After this, the parameters of the $2^+(s=1)$ state were fixed at the experimental values: $E^{2+}=770$ keV, $\Gamma^{2+}=157$ keV. The remaining parameters were varied. The table shows that the quality of the description remained almost the same; the parameters of the 0^+ resonance were unchanged, while those of the 1^- res-

TABLE VI. Parameters of ^{10}Be resonance states near the ^{7}Li+t threshold. The values of E and Γ are given in kilo-electron-volts (laboratory system).

Reaction	Number of parameters	χ^2	1^-		0^+		2^-		2^+	
			E	Γ	E	Γ	E	Γ	E	Γ
^{7}Li(t,α_0)^{6}He	20	41,57	-180	178	174	50	—	—	606	165
	14	41,62	-219	104	173	50	—	—	770	157
^{7}Li(t,α_1)^{6}He*	20	63,78	—	—	165	90	210	21	—	—
	16	68,24	—	—	168	100	206	23	—	—

onance were slightly changed. Figure 4 illustrates the least-squares approximation of the differential S factor of the ^{7}Li(t, α_0)^{6}He reaction by the function (52).

Analysis of the S factor of the ^{7}Li(t, α_1)^{6}He*(2^+) reaction indicated the existence of two resonances of opposite parity in the investigated energy region. One of them, 0^+, has practically the same energy as in the (t, α_0) reaction. However, the width parameters differ by a factor of two. This may be due either to different statistical accuracies of the measurement of the excitation functions [in the (t, α_1) reaction the statistical errors were less] or to the experimental individuation of the resonance [in the (t, α_0) reaction, there were fewer experimental points than in the (t, α_1) reaction]. From both points of view, the data from the (t, α_1) reaction are to be preferred. The negative-parity resonance evidently has $J=2$, since the $J^\pi=1^-$ resonance is outside the investigated energy region, as is indicated by the analysis of the (t, α_0) reaction. The results of the approximation of the S factor of the ^{7}Li(t, α_1)^{6}He*(2^+) reaction by the function (52) are given in Table VI and shown in Fig. 5.

In the analysis of the differential cross section of the ^{7}Li(t, α_1) reaction, the resonance at E_t=260 keV was eliminated because of its poor experimental individuation (just four experimental points in Fig. 5). This resonance is not present in the differential cross section of the ^{7}Li(t, α_0) reaction. Comparing (49) and (50), we can conclude that its quantum numbers must be chosen from the three pairs

$$J^\pi=2^-,1^+,3^+. \tag{53}$$

Confirmation of the existence of the 260-keV resonance can be found in analysis of the differential cross section of the ^{7}Li(t, n) reaction measured[52] at 0 and 90° (Fig. 6). The cross section was described theoretically by means of the function (52) by the least-squares method. The number of neutron channels was more than 20. Therefore, it is not possible to determine the quantum numbers from the available experimental data. We need here measurements of the differential cross sections for the individual channels and at different angles. The analysis in the neutron channel unambiguously indicates a resonance at 260 keV, as can be seen from Fig. 6. The resonance width is estimated at 20 keV, and the quantum numbers are evidently determined by one of the pair of numbers in (53).

Summarizing the analysis of the ^{7}Li(t, α_0), ^{7}Li(t, α_1), and ^{7}Li(t, n) differential cross sections, we can give the following scheme of previously unknown ^{10}Be levels near

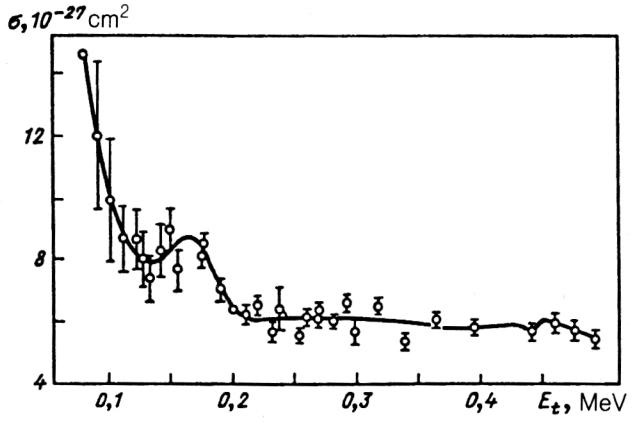

FIG. 4. Theoretical description of differential S factor at angle 90° in the ^{7}Li(t, α_0)^{6}He reaction.

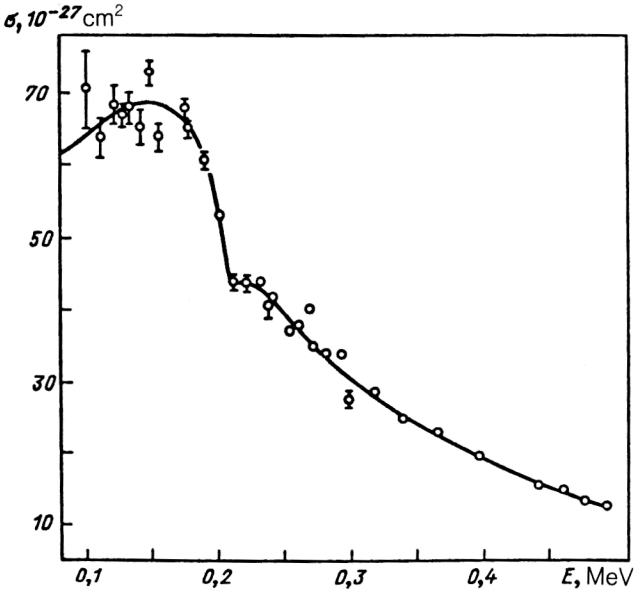

FIG. 5. The same as in Fig. 4 in the ^{7}Li(t, α_1)^{6}He*(2^+) reaction.

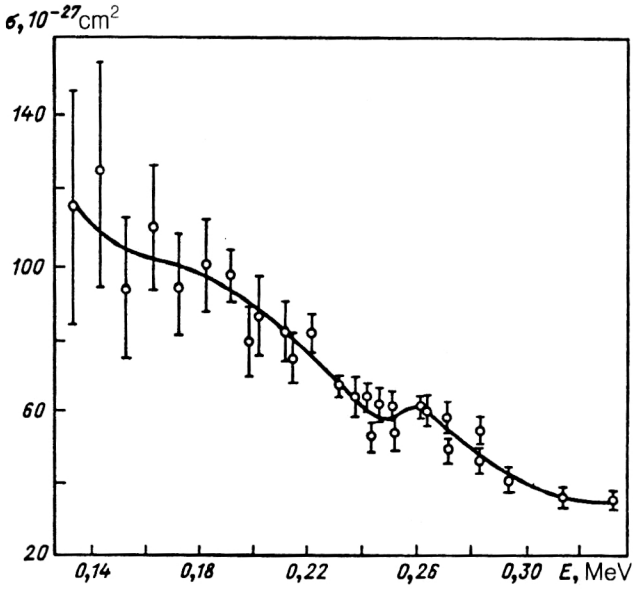

FIG. 6. The same as in Fig. 4 in the ^{7}Li(t, n) reaction.

the threshold E_q=17.2498 MeV of the ^{7}Li+t channel (Table VII). The actual existence of the 1^- (E_x=17.11 MeV) level is in doubt, since it is not found in the experimentally investigated region E_t=80–500 keV. The observed growth of the differential cross sections on the approach to the ^{7}Li+t threshold (see Figs. 4 and 6) need not necessarily be due to the presence of a near-threshold resonance but could also arise from an l=1 partial wave, giving a linear dependence on the energy E_t (52). The theoretical function (52) is defined only above the threshold. It cannot be used for predictions below the threshold.

Phase-shift analysis of proton elastic scattering by ^{7}Li nuclei near two thresholds of the ^{7}Li(p, n)^{7}Be reaction

The theory of resonance threshold phenomena found application[63,64] in phase-shift analysis of ^{7}Li(p, p)^{7}Li differential cross sections measured at proton energies E_p=1.35–3 MeV in the laboratory system[2] at six scattering angles θ: 70, 90, 110, 130, 150, and 167.1° in the center-of-mass system. At proton energies E_q=1.88 MeV and E_q=2.3705 MeV two thresholds of the ^{7}Li(p, n)^{7}Be reaction open, corresponding to production of the ^{7}Be nucleus in the ground and first excited states. The phase-shift analysis is complicated by two circumstances: competing open channels of the (p, p_1), (p, α), and (p, γ) reactions[10] and also the existence of four resonance states of the ^{8}Be compound nucleus shown in Table VIII.[10]

The levels of the ^{8}Be nucleus are measured from the first neutron threshold. The phase-shift analysis made earlier in Ref. 65 using the same experimental data[2] could not be satisfactory because it did not use a theory of threshold phenomena permitting prediction of the energy dependence of physical quantities. It was decided to repeat the phase-shift analysis having made preliminary investigations of the possibilities of adequate description of the experimental data by means of a theoretical function by least-squares variation of parameters.

The original attempt at a theoretical description of the first threshold level and of the 2^- resonance level nearest to it (see Table VIII) in an energy interval containing these two states did not lead to success. A further extension of the energy interval and inclusion, in the theoretical function of the next state of the compound nucleus in this interval improved the description of the experimental data. The best description was achieved when the theoretical function included both threshold states and all four ^{8}Be resonances (Table VIII). These investigations showed that all six states strongly interact with one another. The influence of the ^{8}Be resonances at the ends of the investigated energy interval was ignored. The description of the differential cross section for ^{7}Li+p elastic scattering is given by the expression[23]

$$\frac{d\sigma}{d\Omega_p}=\frac{1}{8}\left|f_c+f_N\right|^2, \tag{54}$$

TABLE VII. Levels of the nucleus ^{10}Be near the threshold of the ^{7}Li+t channel.

E_x, MeV	Γ_{cms}, keV	J^π	T
(17,11 ± 0,02)	(100 ± 30)	1^-	1
17,37 ± 0,01	60 ± 30	0^+	1
17,40 ± 0,005	15 ± 2	2^-	1
17,43 ± 0,005	15 ± 2		1

TABLE VIII. Data on levels of the nucleus ^{8}Be and the corresponding energies of the incident protons E_{pc} (c.m.s.) and E_p (lab).

Level	E_x, MeV	J^π	T	Γ, keV	E_{pc}, MeV	E_p, MeV
1	18,91	2^-	0	48 ± 20	1,656	1,893
2	19,07	3^+	1	270 ± 20	1,816	2,075
3	19,24	3^+	0	230 ± 30	1,986	2,270
4	19,4	1^-	0	~650	2,146	2,453

where 1/8 is a statistical factor. The Coulomb, f_C, and nuclear, f_N, parts of the amplitude can be represented in the form

$$f_c=\frac{\sqrt{\pi}}{k_p}\left[-C_{p'}(\theta_{p'})\right]\delta_{pp'},$$

$$C_p(\theta_p)=\frac{\eta_p}{\sqrt{4\pi}\sin^2(\theta_p/2)}\exp\left\{2i\eta_p\ \ln\sin\frac{\theta_p}{2}\right\},$$

$$f_N=\frac{i\sqrt{\pi}}{k_p}\sum\sqrt{2l+1}Y_{l'm'}(\Omega_{p'})(slv0|JM) \tag{55}$$

$$\times(s'l'v'm'|JM)T^{J^\pi}_{p's'l',psl},$$

$$T^{J^\pi}_{p's'l',psl}=\exp(2i\omega_{p'l'})\delta_{p's'l',psl}-U^{J^\pi}_{p's'l',psl},$$

where Ω_p and θ_p are the solid and polar scattering angles; v, m, and M are the projections of s, l, and J, respectively. The primed quantum numbers correspond to the exit channel. The scattering matrix U and the Coulomb phase ω are determined in (20) and (2), respectively. The general form of the elements of U was specified in the single-channel approximation with allowance for the correction from the multichannel formulas (21) in the form of a redistribution of the real parts of the amplitudes $\mathfrak{M}$ and a in favor of the imaginary parts:

$$U^{J^\pi}_{p's'l',psl}=P^{1/2}_{l'}(E'_p)\left(\mathfrak{M}^{J^\pi}_{s'l',sl}\right.$$

$$\left.+\sum_N\frac{(a^{J^\pi}_N)_{s'l',sl}}{E-E^{J^\pi}_N+i\Gamma^{J^\pi}_N/2}\right)P^{1/2}_l(E_p)$$

$$\times\left[1-\sum_{ns_nl_n}(C^{J^\pi}_n)_{s_nl_nsl}(E-E_{qn})^{l_n+1/2}\right]. \tag{56}$$

Here, the sum over N includes all resonance states of the compound nucleus with the same set of quantum numbers J, π. The sum over n denotes a summation over all threshold energies $E_{q,n}$. In the absence of open channels of the (p, p_1), (p, α), (p, γ) reactions, the coefficients C_n must be real and positive parameters of the coupling of the (p, n) channels; this follows from unitarity. They were taken thus in the calculations of the differential cross sections. In actual fact, the replacement of the multichannel expressions (23) by the single-channel expression (56) can lead to complex values of C_n. A further simplification in the calculations was a restriction to zero orbital angular momenta in the threshold channels. This meant that the threshold states were excited by partial waves with even l equal to 0 and 2, since the mirror nuclei ^{7}Li and ^{7}Be in the ground and first excited states have the same spins and parities, which are $3/2^-$ and $1/2^-$, respectively.[10] The theoretical function describing the energy dependence of the differential cross section (54) contained 28 real parameters. Of these, 20 depended on the scattering angle, and eight were the parameters of the energy E and width Γ of the four ^{8}Be resonances (see Table VIII). We were interested in testing whether the ^{8}Be level parameters were independent of the scattering angle and matched the recommended values given in Table VIII, and also in estimating the quality of the description of the differential cross sections at different angles.

The differential cross section was described theoretically as follows. For each of the six scattering angles, the initial procedure consisted of fixing eight parameters of the ^{8}Be levels at the recommended values (Table VIII) in the theoretical function and varying the remaining 20 parameters by the least-squares method. After the best description had been achieved, the level parameters were made free, and all 28 were varied. This resulted in a significant improvement of the description compared with the case of variation of 20 parameters, though the ^{8}Be level parameters changed little. The results of the least-squares analysis are given in Table IX.

For each scattering angle, this table gives the number of experimental points, the minimum χ^2, the width of the energy interval, and the calculated parameters of the resonances of the ^{8}Be compound nucleus. The experimental accuracy of the data in Ref. 2 is 1–3% depending on the cross section. The values of min χ^2 per point increase on the average from 1.8 for angles 70–110° to 5.3 for 130–167.1°, i.e., the deviation of the calculated curve from the experimental points does not exceed twice the errors. The largest deviation is observed for 167.1°. Figure 7 illustrates the quality of the description of the differential cross section at this angle. It can be seen that the first threshold anomaly is convincingly reproduced by the calculations, while the second is manifested less clearly. There is a good description of the region of strong interference of the isospin doublet of $J^\pi=3^+$ states with $T=1$ ($E=1.801$ MeV) and $T=0$ ($E=1.963$ MeV) in ^{8}Be. It follows from Table IX that the spreads of E_N and Γ_N are small. Thus, the analysis establishes that: 1) the theory is viable and describes adequately the experimental data in the case of interaction of two threshold and four resonance states of the ^{8}Be compound nucleus in a 1-MeV energy interval; 2) the parameters of the compound-nucleus resonances do not depend on the scattering angle and agree with the recommendations[10] within the above accuracy; 3) the doublet of 3^+ levels is shifted downward by 15–20 keV, this being attributable to the neglect of $l_n=1$ threshold states excited by partial waves with odd l_p equal to 1 and 3. According to our data, a "threshold" level (18.91 MeV, $J^\pi=2^-$, $T=0$) is situated 10 keV above the neutron threshold to the ^{7}Be ground state and is an ordinary quasi-stationary state of the ^{8}Be nucleus. This conclusion agrees with the observation of a resonance at $E=1.658$ MeV ($\Gamma=50$ keV) in the ^{7}Li(p, γ)^{8}Be*(16.6 and 16.9 MeV)$\rightarrow 2\alpha$ reaction cross section[10] but not with the hypothesis that this state is virtual,[66] i.e., lies below the threshold ($Q_{pn_0}=1.646$ MeV). Such a conclusion was based on analysis of the energy dependence of the ^{7}Li(p, n_0)^{7}Be reaction cross section and the $^5S_2$ phase shift[60] near the threshold in the scattering-length approximation. The estimate of the width ($\Gamma=50$ keV) is close to our value. Note that the position

TABLE IX. Parameters of resonances from analysis of differential cross sections for elastic scattering of protons by ^{7}Li. The energies are given in the center-of-mass system.

Parameter	Scattering angle (in c.m.s.), deg							Data of Ref. 10
	70	90	110	130	150	167,1	Mean	
No. of points	74	97	73	79	69	73	—	—
$\min \chi^2$	107	263	92	306	319	545	—	—
E_p, MeV	1,18–2,23	1,17–2,62	1,18–2,28	1,18–2,64	1,18–2,3	1,18–2,42	—	—
E^{2-}, MeV	1,654	1,650	1,657	1,654	1,664	1,670	1,654	1,656
Γ^{2-}, keV	49,6	47,8	48,6	48,0	74,0	75,2	48,5	48±20
E_2^{3+}, MeV	1,802	1,804	1,809	1,803	1,789	1,796	1,801	1,816±0,03
Γ_2^{3+}, keV	281	301	275	290	318	301	295	270±20
E_3^{3+}, MeV	1,965	1,965	1,959	1,964	1,950	1,978	1,963	1,986±0,025
Γ_3^{3+}, keV	211	206	210	208	191	194	203	230±30
E^{1-}, MeV	2,145	2,146	2,142	2,144	2,147	2,149	2,145	2,146
Γ^{1-}, keV	651	637	636	649	641	626	640	~650

of the S-matrix pole (42 keV from the real axis in the complex energy plane) corresponds to a Breit–Wigner width 84 keV. If the resonance with width 46 keV that we have found were virtual, then it would lie 24 keV below the threshold, i.e., 34 keV lower than was found in the description of the experiment. The discrepancy in the position of the 2^- state can be attributed to the difference between the theoretical approaches to the description of the same data.

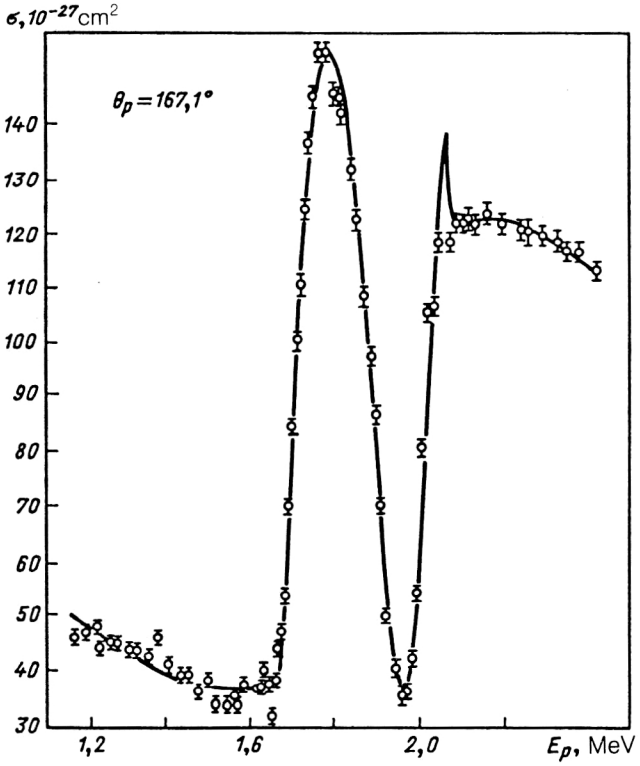

FIG. 7. Theoretical description of excitation function in ^{7}Li$(p, p)^7$Li scattering at angle 167.1°.

A second "threshold" ^{8}Be state (19.4 MeV, 1^-) is manifested near a second threshold ($Q_{pn_1} = -2.073$ MeV) but very weakly, this evidently reflecting the weakness of the resonance enhancement, which depends on Γ_p/Γ. The total width $\Gamma = 650$ keV is 13 times greater than at the first resonance because of the growth of the neutron width Γ_{n_0} in the open channel. With Γ_p unchanged, the enhancement effect decreases rapidly because of the large growth of $\Gamma = \Gamma_p + \Gamma_{n_0} + \Gamma_{n_1}$. After the preliminary investigation of the differential cross section for elastic scattering of protons by ^{7}Li nuclei, a phase-shift analysis of the scattering was made. The successful solution of this problem depended to a large degree on the correct choice of the parameters in the theoretical function. The parameters must satisfy the following conditions: 1) they must be independent of the angle and energy variables; 2) they must be mutually independent; 3) the number of parameters must be minimal. The problems of mutual independence of the parameters and independence of the angle variables was solved by Seyler.[65,67] Independence of the energy was solved by expanding the parameters in powers of the energy near the neutron thresholds, and the minimum number of parameters is determined by the physical formulation of the problem and the technical capabilities of the computer.

For incident-proton energies $E_p < 3$ MeV, it is sufficient to consider partial waves with $l_p \leqslant 2$. The channel spin takes two possible values: $s = 1$ and 2. Under these conditions not more than three elastic-scattering channels correspond to a definite set of numbers J, π, this being a consequence of the triangle law for addition of the angular momenta l and S and of parity conservation. In accordance with Refs. 65 and 67, the matrix of elastic scattering can be represented in terms of intrinsic phase shifts δ^{J^π} and real orthogonal matrices u^{J^π}:

$$U^{J^\pi}_{c(m),c(n)}=\sum_{p'=1}^{3} u^{J^\pi}_{pm}u^{J^\pi}_{pn}\exp(2i\delta^{J^\pi}_{c(p)}), \tag{57}$$

where $c(i)$ is the channel label determining the combination of numbers s_i and l_i in the ith intrinsic phase $\delta_{c(i)}$. The matrices u^{J^π} are given in terms of the mixing parameters ε, ζ, and η:

$$\begin{aligned}
&u_{11}=\cos\eta\cos\zeta, \quad u_{12}=\sin\eta\cos\zeta, \quad u_{13}=\sin\zeta,\\
&u_{21}=-\cos\varepsilon\sin\eta-\sin\varepsilon\sin\zeta\cos\eta,\\
&u_{22}=\cos\varepsilon\cos\eta-\sin\varepsilon\sin\zeta\cos\eta, \quad u_{23}=\sin\varepsilon\cos\zeta,\\
&u_{31}=\sin\varepsilon\sin\eta-\cos\varepsilon\sin\zeta\cos\eta,\\
&u_{32}=-\sin\varepsilon\cos\eta-\cos\varepsilon\sin\zeta\sin\eta, \quad u_{33}=\cos\varepsilon\cos\zeta.
\end{aligned} \tag{58}$$

The parameter ε mixes the channel spins s without mixing the orbital angular momenta l; ζ mixes l without mixing s; η couples partial waves with different l and s.

When there are only two elastic-scattering channels for given J^π with possible mixing of the spin channels, Eq. (57) can still be used if the term with $p=1$ in it is set equal to zero and $\eta=\zeta=0$ in Eqs. (58). If only one elastic-scattering channel is possible, then $U=\exp(2i\delta)$ for this channel. An exception is the case $J^\pi=3^+$, for which in one channel (s, $l=2$, 1) there exists a doublet of states of the ^{8}Be compound nucleus with $T=1$, 0. In accordance with the theory of nuclear reactions, (20) and (23), the corresponding element of the scattering matrix can be represented in the form of two terms:

$$U^{3^+}_{21,21}=\frac{1}{2}\sum_{N=2,3}\exp(2i\delta^{3^+}_{21,N}). \tag{59}$$

Using the relations (21), we find the energy dependence of the intrinsic phase shifts:

$$\delta^{J^\pi}_{c(p)}=\Delta^{J^\pi}_{c(p)}+\delta^{J^\pi}_{c(p),N}+\frac{i}{2}\sum_n a^{J^\pi}_{c(p),n}(E-E_{qn})^{l+1/2}\times\left[1+\frac{1}{3}(a^{J^\pi}_{c(p),n})^2(E-E_{qn})\delta_{l0}\right], \tag{60}$$

where $\delta^{J^\pi}_{c(p),N}$ is the phase shift of the resonance scattering, and

$$\delta^{J^\pi}_{c(p),N}=\arctan\frac{\Gamma^{J^\pi}_N}{2(E^{J^\pi}_N-E)}. \tag{61}$$

In the absence of a resonance for the set of J^π numbers, the contribution of the resonance phase is set equal to zero.

The phase shifts (60) represent an expansion of the function of the energy in powers of E up to $E^{3/2}$, since the threshold states with $l=0$ and 1 are taken into account. Therefore, the potential-scattering phase shift Δ^{J^π} is a linear (entire) function of the energy. To reduce the number of parameters, it was decided to take Δ^{J^π} to be a constant, averaged over the energy interval. The parameters a^{J^π} of the coupling of the (p,n) channels are real constants. Our approach and the approach of Ref. 65 to the problem of phase-shift analysis are similar in giving the description in terms of the intrinsic phase shifts δ and the real orthogonal matrices u^{J^π}. However, there are important differences in the two approaches. In Ref. 65, the phase shifts were least-squares varied as unknown functions of the energy. In our work, the energy dependence of the phase shifts is determined theoretically, and the parameters Δ, a, ε, ζ, and η, which are in fact constants, are varied. In addition, in Ref. 65 the ^{8}Be doublet with $J^\pi=3^+$ and $T=1$, 0 is described by the single phase shift $\delta^{3^+}_{21}$ ($^5P_3$). We describe the doublet by two phase shifts $\delta^{3^+}_{21,N}$, where N is equal to 2 and 3. In Ref. 65, the contribution of the competing (p, n), (p, p_1), and (p, α) reaction channels was taken into account by the introduction of imaginary parts in the intrinsic phase shifts δ, and the imaginary parts were also varied. In our work, the contribution of the (p, n) reaction channels, which makes the largest contribution, is taken into account exactly by the introduction, in the phase shifts (60), of the threshold energy dependence with parameters a^{J^π}. The contribution of the (p, p_1), and (p, α) reaction channels is specified numerically as follows. Near the first neutron threshold, unitarity is used to calculate the absolute value of the corresponding elements of the scattering matrix on the basis of the known cross sections of these reactions. Thus, for the (p, p_1) reaction it was found that $|U^{1^-}_{p10,p10}|^2=0.467$, from which it follows that the matrix element $U^{1^-}_{p10,p10}$ must be multiplied by 0.730. At the same time, it is assumed that the energy dependence of the phase shift (60) does not change. It remains an open question whether the (p, p_1) reaction channel influences the other elements of the scattering matrix. The angular-momentum and parity conservation laws do not forbid it. Our restriction to a single element $U^{1^-}_{p10,p10}$ is merely a plausible assumption, given the weak anisotropy in the angular distribution of protons p_1 (Ref. 68). A similar assumption was made in Ref. 65. It is more complicated to determine the contribution of the (p, α) channel. Because of the strong anisotropy in the α-particle angular distribution,[69] it is necessary to take into account orbital angular momenta l equal to 0 and 2. From the differential cross section of the (p, α) reaction the absolute values of the elements of the reaction matrix cannot be determined uniquely. We therefore first found limits on the variation of their values and then chose mean values. In determining the absolute values of the elements of the scattering matrix by means of the unitarity relation, we made essential use of the fact that the parameter ε^{2^+} of the mixing of the channel spins vanishes. As a result, we chose the absolute values

$$|U^{0^+}_{11,11}|^2=0.837, \quad |U^{2^+}_{11,11}|^2=0.933, \quad |U^{2^+}_{21,21}|^2=0.98. \tag{62}$$

In Ref. 65, only the one phase shift $\delta^{0^+}_{11}$ was subject to influence of the (p, α) reaction. In both Ref. 65 and our work, the influence of the (p, γ) reaction on the phase shifts was ignored. In place of the numbers (62), one could introduce additional varied parameters into the corresponding phase shifts. We rejected this approach to avoid overburdening the already complicated problem. The

TABLE X. Parameters of phase shifts.

J^π	s, l	$\Delta_{sl}^{J\pi}$	$a_1^{J\pi}$	$a_2^{J\pi}$	$\varepsilon^{J\pi}$	$\zeta^{J\pi}$	$\eta^{J\pi}$
0^-	2,2	−0,08	—	—	—	—	—
0^+	1,1	0,277	−0,414	−1,211	—	—	—
1^-	1,0	−1,367	0,956	0,122	—	—	—
	2,2	−1,841	—	—	−1,35	−0,8	−0,14
	1,2	−2,152	—	—	—	—	—
1^+	1,1	−0,576	−0,181	0,89	1,565	—	—
	2,1	0,263	−0,278	—	—	—	—
2^-	2,0	−4,666	0,048	—	—	—	—
	1,2	0,048	—	—	3,06	0,23	1,56
	2,2	0,254	—	—	—	—	—
2^+	1,1	0,149	0,536	−4,106	−0,036	—	—
	2,1	−0,202	−2,159	—	—	—	—
3^-	2,2	0,181	—	—	1,17	—	—
	1,2	0,0053	—	—	—	—	—
3^+	2,1	1,335	−2,027	—	—	—	—
	2,1	−1,569	1,628	—	—	—	—
4^-	2,2	−0,064	—	—	—	—	—

Note: Here Δ, ε, ζ, and η are measured in rad, $a_1^{J^-}$ in $\text{MeV}^{-1/2}$, and $a_2^{J^+}$ in $\text{MeV}^{-3/2}$.

phase shifts contain 17 parameters Δ, 13 parameters a of the coupling of the (p, n) channels, and nine mixing parameters ε, ζ, η. If necessary, the resonance parameters E and Γ, for $N=1$–4, can also be varied.

Table X gives all 39 parameters of the phase shifts obtained as a result of the best description of the differential cross section for $^7\text{Li}(p, p)^7\text{Li}$ scattering.

It follows from Table X that the potential-scattering phase shifts Δ are small in absolute magnitude for $l=1$ and 2, which is a natural result for the considered low-energy incident protons. An exception is the case of states with J^π equal to 1^- and 3^+. For the case with $J^\pi=1^-$, this can be attributed to incorrect allowance for the competing (p, p_1) reaction channel; in accordance with the unitarity relation for the scattering matrix, we concentrated its effect on the single elastic-scattering matrix element $U_{10,10}^{1^-}$. The angular momentum and parity conservation laws made it possible to distribute the effect over 14 matrix elements. The other exception, in the case with $J^\pi=3^+$, arises because the states of the isotopic doublet with $T=1, 0$ interact strongly with each other. The difference $\Delta_{22}^{T=1}-\Delta_{21}^{T=0}=2.9$ is near π, indicating strong interference of them. Separate analysis of the phase shifts for positive and negative parities shows the following. For $\pi=(-)$ and $l=2$, we have $\Delta_{22}^{J^-} > \Delta_{12}^{J^-}$, i.e., the potential scattering is stronger in the state with parallel spins of the proton and target nucleus $(s=2)$ than in the state with antiparallel spins $(s=1)$. For given J^-, the signs of the phase shifts $\Delta_{22}^{J^-}$ and $\Delta_{12}^{J^-}$ are the same. The phase shifts with $l=0$ are negative and large in absolute value, as is characteristic of S-wave phase shifts. For $\pi=(+)$, the phase shifts with parallel and antiparallel spins have opposite signs: for $s=1$, positive signs correspond to even J and negative signs to odd J. For $s=2$, this correspondence is reversed.

We now consider the mixing parameters ε, ζ, and η. In all states apart from 2^+, there is strong mixing of waves with different spins. Only $\varepsilon^{2^+}=0$. This fact was used in distributing the influence of the (p, α) channel over the elements of the elastic-scattering matrix (62) with $J^\pi=2^+$. The values of the ζ parameters, which mix states with different orbital angular momenta, indicate that noncentral forces play an important part in the $p+^7\text{Li}$ channel, although the ^8Be compound nucleus is an even–even nucleus and the contribution of the tensor forces must be minimal. It is interesting to note that all three mixing parameters in the state $J^\pi=1^-$ have negative sign, and in the state 2^- positive sign.

For the study of nuclear reactions, the parameters of the coupling of analog (p, n) channels are very interesting. Although there is no simple connection between them and the cross section (amplitude) of the $^7\text{Li}(p, n)^7\text{Be}$ reaction, this cross section can be calculated. In addition, the parameters of the coupling of the (p, n) channels make it possible to estimate the effective sizes of the nucleus in the neutron threshold states. From the maximum values of a^{J^π} in Table X, we find that the effective sizes for the ^8Be nucleus can exceed the value in the ground state by a factor of 1.5 for the S threshold and 3 for the P threshold.

We compare the results of the phase-shift analysis with the results obtained in Ref. 65. The S phase shifts $\delta_{20}^{2^-}$ and $\delta_{10}^{1^-}$ in Ref. 65 are not resonance quantities. The phase shift $\delta_{20}^{2^-}$ has a cusp in the region of the first neutron threshold. In the remaining region of energies both of the S phase shifts are practically constant, near zero. In our calculations, the S phase shifts have large negative values, increase by π in the region of the resonances, and at the points of the neutron thresholds undergo a "break" $\sim(E-E_q)^{1/2}$ in accordance with the relation (60). The D phase shifts are constant in the states $J^\pi=0^-$, 3^-, 4^-, while in the states

with $J^{\pi}=2^-$, 1^- they have resonance values. None of them have threshold singularities. The D phase shifts are not given in Ref. 65.

Comparison of the P phase shifts shows that in Ref. 65 the two P phase shifts $\delta_{21}^{2^+}$ and $\delta_{21}^{3^+}$ have anomalous behavior. For $\delta_{21}^{2^+}$, this is evidently due to the neglect of the contribution of the (p, α) reaction channel to the 2^+ state. The irregularity of the P phase shift in the 3^+ state is due to interference of the two levels of the isotopic doublet with $T=1$ and 0, although it is described in Ref. 65 by one phase shift instead of two. In our work, the P phase shifts are $\sim(E-E_q)^{3/2}$, and for the 3^+ isotopic doublet are also resonance in nature. It is interesting to compare our results with those of the phase-shift analysis of $\alpha\alpha$ scattering made in Ref. 70. In the phase shifts δ_0, δ_2, and δ_4 one can clearly see threshold anomalies at $E=39$ MeV corresponding to the first and second neutron thresholds. The threshold anomalies in δ_0 and δ_2 are due to P threshold states, and in δ_4 to an F threshold state ($l=3$). These experimental data indicate a significant influence, on the phase-shift analysis, of not only threshold states with $l=0$ but also those with high angular momenta.

The difference between our phase shifts and those of Ref. 65 is explained not only by the different approaches but also by the number of phase shifts in which the scattering channels and different projections are taken into account. For comparison, we give these numbers for our work and for Ref. 65, respectively: 17 and 16 in the (p, p) reaction, nine and three in the (p, n) reaction, three and one in the (p, α) reaction, and one and one in the (p, p') reaction.

The numerical values of the phase shifts given in Table X were used to calculate the polarization of protons scattered elastically by ^{7}Li nuclei through angles 70, 90, 110, 130, and 150°. The experimental values of the polarization for the same angles are given in Ref. 65. The calculations give qualitative agreement of the theory and experiment at angles 70–90°. With increasing angle and decreasing importance of Coulomb scattering, the agreement becomes qualitative, indicating adequacy of the theory and sufficiently reliable estimates of the parameters of the "nuclear" scattering. Figure 8 shows calculations of the polarization at 150°. The broken curve shows the calculations of the polarization with allowance for only S threshold states. It is clear that they do not correspond to the experiment. In our view, the last result is unexpected, since in the threshold channel and in the elastic-scattering channel the contribution from the P waves is small, except for the resonance 3^+ states of the isotopic doublet. The coupling of the (p, n) channels in the $l=1$ state radically changes the polarization of the protons in the elastic channel.

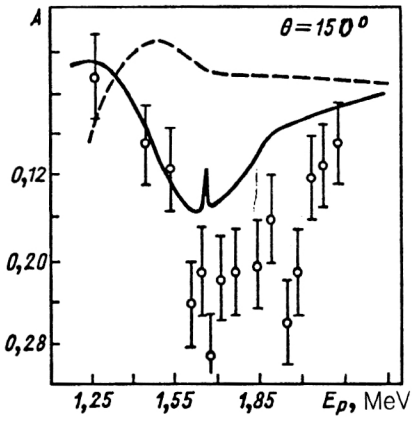

FIG. 8. Analyzing power in elastic scattering of polarized protons by ^{7}Li nuclei at angle 150°.

Investigation of few-nucleon systems by the resonating-group method

The resonating-group method is successfully used to analyze nuclear structure and to describe the cross sections of nuclear reactions near thresholds in few-nucleon systems[37–42] in the region of excitation energies ~20 MeV. In Ref. 37 a study was made of the continuous spectrum of the ^{4}He nucleus between the thresholds of the $p+T$ and $n+^3$He reactions and of the 0^+ resonance with energy 0.3 MeV above the $p+T$ threshold. It was shown that in the single-channel approximation ($p+T$ channel) there is no 0^+ resonance. Inclusion of a closed neutron channel leads to the appearance of the 0^+ resonance with width $\Gamma^{0^+}=1.63$ MeV (experimental value $\Gamma_{\text{exp}}=0.27$ MeV). After allowance for a third, closed $d+d$ channel, the theoretical parameters of the resonance, $E^{0^+}=0.12$ MeV and $\Gamma^{0^+}=0.26$ MeV, were close to the experimental values. Therefore, the redistribution of the wave-function amplitudes (62) between the pT, n^3He, and dd channels helps the formation of the 0^+ resonance. This resonance is satisfactorily described by the singlet phase shift. The triplet phase shift is much smaller. Representation of the phase shift at the threshold of the neutron channel in accordance with the theory of threshold phenomena in the form of the series

$$\delta_0(e)=\delta_0^{(0)}-A(E-E_q)^{1/2}$$

makes it possible to calculate the imaginary part of the singlet scattering length for neutron scattering by ^{3}He and, therefore, to find the effective cross section for capture of thermal neutrons by the ^{3}He nucleus. Calculations were made with the Hasegawa–Nagata potential and in the three-channel approximation satisfactorily describe the known experimental data on $p+T$ and $n+^3$He interactions in the region between the thresholds of these channels and somewhat above the $n+^3$He threshold.

Thus, the Coulomb barrier in the $p+T$ channel cannot ensure the appearance of a resonance state. The 0^+ resonance is formed under the influence of the dynamics of the three coupled channels (pT, n^3He, dd) of decay of the ^{4}He nucleus. In Ref. 38, it is asserted that the 0^+ resonance is a superposition of simple $1p$–$1h$ excitations.

The $3^+/2$ resonance of the ^{5}He compound nucleus and of its mirror nucleus ^{5}Li have different properties. Calculations of the cross sections of the mirror reactions $d(T, n)$

and $d(^3\text{He}, p)$ at below-barrier energies using the Hasegawa–Nagata potential are given in Refs. 39 and 40. In the single-channel $d+T(^3\text{He})$ approximation, the phase shift δ_1 has a pronounced resonance behavior, reflecting penetration of the colliding nuclei into the region of the compound nucleus. Allowance for coupling with the exit channel does not lead to a qualitative change of δ_1. At the same time, the coupling of the entrance and exit channels significantly changes the behavior of δ_2 in the exit channel $n+\alpha(p+\alpha)$. In the single-channel approximation, δ_2 is practically constant. Allowance for the channel coupling leads to a strong energy dependence of δ_2 and indicates a resonance behavior of it. The parameters of the resonance (energy and width) increase with allowance for channel coupling, since the presence of a second open channel effectively decreases the Coulomb barrier, allowing the system to break up through this channel. Calculations of the energy dependence of the $d(T, n)\alpha$ and $d(^3\text{He}, p)\alpha$ reaction cross sections agree well with the experimental data. The values of the astrophysical S factor at zero energy were also calculated. As a result of the calculations it may be concluded that the existence of the $3^+/2$ resonance is due to the Coulomb barrier in the entrance channel. This is confirmed by an analysis of the wave functions in which the ratio of the squares of the amplitudes of the wave functions of the $d+t$ and $n+\alpha$ channels is calculated. It has the order 10^2–10^3 in the region of the resonance energy.

In Ref. 40, experimental data on the $^3\text{He}(d, p)\alpha$ and $^3\text{H}(d, n)\alpha$ reactions[71] with polarized deuterons at low near-threshold energies were analyzed. The resonating-group method was used to calculate the components T_{20}, T_{21}, T_{22}, and T_{11} of the polarization tensor. Except for T_{11}, all components agree well with the experimental values. The amplitude of T_{11} is half the experimental value in the region of the $3^+/2$ resonance at 430 keV (laboratory system). This means that not only the partial wave $l=0$ but also waves with $l=1$ and 2 contribute to the resonance.[40] Thus, it is shown that the $3^+/2$ resonance has an admixture of positive-parity states. For the $^3\text{H}(d, n)\alpha$ reaction, this admixture is smaller.

In Ref. 41, a study was made of the mechanism of isospin conservation in the $^4\text{He}(d, ^3\text{He})T$ reaction with polarized deuterons in the energy interval from the reaction threshold and above: 14–33 MeV (center-of-mass system). An improved resonating-group method was used to calculate the differential cross section and the component $T_{11}(\theta, E)$ of the polarization tensor in order to verify the Barshay–Temmer theorem $\sigma(\theta)=\sigma(\pi-\theta)$. The nonconservation of isospin is 5–10% and arises from the coupling to an intermediate $5+1$ structure in a two-step mechanism of nucleon transfer.

In Refs. 42 and 72, the resonating-group method was used to study the seven-nucleon system. In Ref. 42, the astrophysical S factor of the $^3\text{H}(\alpha, \gamma)^7\text{Li}$ and $^3\text{He}(\alpha, \gamma)^7\text{Be}$ reactions at $E=0$ was calculated in the framework of the algebraic version of the method.[6] One open channel was taken into account. The influence of closed channels was ignored. The nucleon-nucleon potential used was the potential MHN,[36] whose parameters were chosen to reproduce accurately the experimentally observed parameters of the ^7Li and ^7Be nuclei. The variational conditions of stability for each of the clusters are not satisfied separately. The values obtained for the S factor,

$$S(0)=69\cdot 10^{-26}\ \text{cm}^2\cdot\text{keV}(^7\text{Be}),$$

$$S(0)=15.5\cdot 10^{-26}\ \text{cm}^2\cdot\text{keV}(^7\text{Li}),$$

exceed somewhat the results of extrapolation of the experimental data and agree with the estimate given in Ref. 73. Calculations of $S(0)$ were also made in Ref. 74 in the framework of a simple cluster model in which the clusters are assumed to be structureless. The interaction between them is modeled by a local potential of Gaussian form. The Coulomb interaction corresponds to interaction of a point charge with a uniformly charged sphere of finite radius. The values of the $S(0)$ factor obtained in Ref. 74 are approximately 30% smaller than the values of $S(0)$ obtained in Ref. 42. The discrepancy evidently arises because the parameters of the model of Ref. 74 were chosen to give the best description of the parameters of the free clusters α, ^3He, and ^3H.

The differential cross section $\sigma(\theta, E)$ for elastic scattering of polarized protons by ^6Li nuclei in the interval of energies from the threshold of the $^6\text{Li}(p, \alpha)^3\text{He}$ reaction and above, namely, 1.6–10 MeV, was calculated in Ref. 72. A group of four resonances $(1/2, 3/2, 5/2)^-$ in ^7Be at excitation energies 9–13 MeV was predicted. Phase-shift analysis of the experimental data of Ref. 75 using the cross section $\sigma(\theta, E)$ and the vector analyzing power $A(\theta, E)$ made in Ref. 72 confirmed the existence of four broad overlapping resonances in the energy region considered in Ref. 72.

We give a summary of calculations, by the resonating-group method of the dynamics of nuclear reactions in two-nucleon systems in a threshold energy region. The far from complete list of studies gives a picture of the wide group of problems that can be solved by this method. We note that the resonance states 0^+ in ^4He and $3^+/2$ in ^5He and ^5Li near the thresholds have shell-filling schemes $(1s)^3(2s1d)^1$ and $(1s)^4(2s1d)^1$, respectively, leaving the $1p$ shell empty. Structurally, the nucleus is a core plus a distant nucleon.

Dispersion-theory study of threshold resonances in the $^{10}\text{Be}(p, n)^{10}\text{B}$ reaction

Measurements of the excitation function of the $^{10}\text{Be}(p, n)^{10}\text{B}$ reaction at energies $E_p<2$ MeV of the incident protons are given in Ref. 77. At energy $E_p=0.248$ MeV, the first neutron threshold opens, and at $E_p=1.039$ MeV the second one opens. Above the second neutron threshold, neutrons from the two (p, n_0) and (p, n_1) reaction channels were detected simultaneously. In the interval of energies $E_p=1.039$–1.4 MeV several (four or more) previously unknown resonances with widths ~ 50 keV and amplitudes differing from one another by not more than 30% were found. These resonances are at the position of the known S level of the ^{11}B nucleus with excitation energy 12.56 MeV and width 210 ± 20 keV (see Fig. 9).[10] The resonances are interpreted in Ref. 48 as threshold P resonances of the ^{11}B

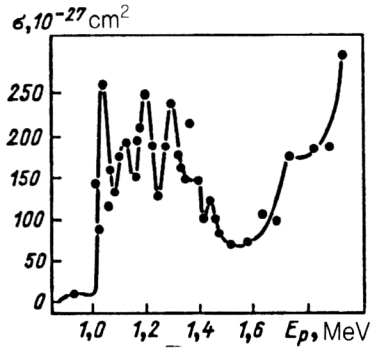

FIG. 9. Neutron yield in the ^{10}Be$(p, n)^{10}$B reaction.

nucleus in the ^{10}Be$(p, n_1)^{10}$B reaction (E_x=0.7184 MeV, 1^+). According to the data of Ref. 48, two resonance states with channel spins 1/2 and 3/2 are formed in the $n+^{10}$B(1^+) system. Each of them is split into two with J values 1/2 and 3/2. As a result, four P resonances are formed. If this interpretation is accepted, it is easy to calculate the ratios of the amplitudes of the P resonances. The total width of the resonances is equal to the sum of the partial widths in the p, n_0, n_1, α, t, γ channels, and only the partial width $\Gamma_{n_1} \sim E_n^{3/2}$ has a strong energy dependence in the region of the second neutron threshold. The total width Γ and all the remaining partial widths in the threshold region of energies E_p=1.039–1.4 MeV are weak functions of the energy, and $\Gamma \gg \Gamma_{n_1}$. In this case, the ratio of the amplitudes of the resonances is determined by the ratio of the partial widths Γ_{n_1} at the energies corresponding to the energies of the resonances. According to the data of Ref. 48, for J=3/2 it is necessary to calculate the ratio of the amplitudes of the third and the first resonances. It is

$$\frac{\Gamma_{n_1}(175 \text{ keV})}{\Gamma_{n_1}(30 \text{ keV})}=\left(\frac{175}{30}\right)^{3/2} \cong 14.$$

This estimate contradicts the results of the experiment.[77] Therefore, in our view the interpretation of the nature of the four resonances given in Ref. 48 cannot be maintained. One may suppose that the broad S resonance of ^{11}B (12.56 MeV) is fragmented into narrow S resonances (Fig. 9), or that its nature is more complicated, the narrow resonances having different natures and different parities (for example, a mixture of S and P resonances). At the same time, not all of them need be threshold resonances. The phase-shift analysis of elastic scattering of protons by ^{10}Be nuclei currently made[78] has shown that the resonance structures observed in the elastic scattering are analogous to the structures in the neutron channel. It may be hoped that phase-shift analysis will clarify the physical nature of the levels of the nucleus near the second neutron threshold.

6. OPEN PROBLEMS OF THEORY AND EXPERIMENT IN THRESHOLD REGIONS

Investigations of threshold phenomena in the framework of model-free theories of nuclear reactions have been made in the region of a neutron threshold or above the threshold of charged particles. At the present time, it is not possible to advance into the below-threshold region of charged-particle production because of the insufficiency of the theoretical investigations of this question. Preliminary investigations for charged particles of the same sign ($Z_1Z_2>0$) were made in Refs. 1, 3, 79, and 80 in R-matrix theory. The case of oppositely charged particles ($Z_1Z_2<0$) was investigated fairly fully in Ref. 4. In the unified theory of nuclear reactions, these questions have not been studied. They must be considered in order to extend the set of studied threshold phenomena. Energy thresholds with the production of charged particles constitute a more numerous and varied family of phenomena than neutron thresholds. Interest in the interaction cross sections of slow charged particles ($E<1$ MeV) arose originally in connection with the investigation of physical processes within stars.[81] At the present time, the interest has shifted to a large degree to energies $E<1$ keV in connection with the problem of cold fusion.[82] Theoretical determination of the energy dependence of the wave function and cross section above and below a threshold will make it possible to extrapolate an experimentally measured cross section to the region of theoretical determination of the cross section. The cross section extrapolated to the region of zero energy will describe the interaction of "bare" charges. Here, we shall not discuss questions associated with electron screening of charges and the influence of other factors interesting from the point of view of cold fusion.

Another important unresolved problem is that of the reliability of the numerical values of the wave-function parameters obtained by least-squares theoretical analysis of excitation functions. The complicated energy dependence of a wave function leads to a strong correlation of the parameters. The existing methods of statistical analysis, including the least-squares method, have a theoretical basis for linear problems and errors of measurement with a normal distribution.[51] In the analysis of threshold phenomena, the excitation function depends linearly on the parameters in power terms with respect to the energy. The parameters occur nonlinearly in the resonance dependence on the energy. The problem of phase-shift analysis is also nonlinear. Nevertheless, all problems of the statistical analysis of threshold phenomena can be classified (there are not more than three of them, as follows from Sec. 3) and investigated theoretically.

CONCLUSIONS

The investigation of threshold phenomena has only begun. One is acutely aware of the lack of proper experimental data (see the discussion of complete experiments in Sec. 3). In our view, two of the most promising theoretical methods of analysis are Feshbach's model-free unified theory of nuclear reactions and the resonating-group method. These methods complement each other. From the analysis of the experimental data by means of the model-free theory one determines the physical parameters of the system, including the channel-coupling parameters, needed in the model theory to select the wave-function subspace in the

resonating-group method. The information about the wave function extracted in the analysis of the threshold phenomena by means of the model-free theory must be compared with the analogous information obtained in theoretical model calculations in order to test the two sets of results against each other and to justify the model assumptions.

Light nuclei are the most convenient objects for investigating threshold states and levels because of the possibility of energy resolution of each of them separately. In medium and heavy nuclei, such possibilities rarely exist (see Sec. 1).

The requirements on the experimental data are as follows. The excitation functions must be measured simultaneously in all open reaction channels with an error not more than 3–5%. The number of experimental points must be approximately 100 in the threshold region $E_q \pm 0.5$ MeV. The energy resolution must be $\Delta E \approx 10$ keV.

In the theoretical analysis, it is necessary to take into account the influence of all open reaction channels. Contrary to the existing opinion,[1,3,4] one must take into account not only the partial waves with minimum orbital angular momentum ($l=0$) in the threshold channel, but also, waves with opposite parity and with higher l. As a rule, the levels of light nuclei nearest the neutron threshold have large reduced neutron widths. The structure of the nucleus in a threshold state can be represented in the core + neutron form. The "outer" neutron is in the $2s1d$ shell, despite a vacancy in the $1p$ shell.

During the last 25 years, nuclear reactions in non-Soviet laboratories have been made mainly with polarized beams and targets. These experiments meet the requirements of a complete experiment to the greatest extent. We hope that in the coming years experiments with polarized particles will become normal in the laboratories in this country too.

[1] E. P. Wigner, Phys. Rev. **73**, 1002 (1948).
[2] P. R. Malmberg, Phys. Rev. **101**, 114 (1956); A. B. Brown, C. W. Snyder, W. A. Fowler, and C. C. Lauritsen, Phys. Rev. **82**, 159 (1951).
[3] G. Breit, Phys. Rev. **107**, 1612 (1957).
[4] A. I. Baz', Ya. B. Zel'dovich, and A. M. Perelomov, *Scattering, Reactions and Decay in Nonrelativistic Quantum Mechanics*, transl. of 1st Russ. ed. (Israel Program for Scientific Translations, Jerusalem, 1966) [Russ. original, 2nd ed., Nauka, Moscow, 1971].
[5] H. Feshbach, Ann. Phys. (N.Y.) **5**, 357 (1958); **19**, 287 (1962).
[6] G. F. Filippov and I. P. Okhrimenko Yad. Fiz. **32**, 932 (1981); **33**, 928 (1981) [Sov. J. Nucl. Phys. **32**, 480 (1980); **33**, 488 (1981)].
[7] G. F. Chew, *The Analytic S-Matrix* (Benjamin, New York, 1966) [Russ. transl., Mir, Moscow, 1968].
[8] S. Mandelstam, Phys. Rev. **112**, 1344 (1958); **115**, 1741 (1959).
[9] L. M. Lazarev, Izv. Akad. Nauk SSSR, Ser. Fiz. **51**, 171 (1987).
[10] F. Ajzenberg-Selove, Nucl. Phys. **A413**, 1 (1984); **A433**, 1 (1985); **A360**, 1 (1981); **A375**, 1 (1982); **A392**, 1 (1983).
[11] S. N. Abramovich, B. Ya. Guzhovskii, A. V. Ershov, and L. M. Lazarev, Izv. Akad. Nauk SSSR, Ser. Fiz. **50**, 2021 (1986).
[12] S. N. Abramovich, B. Ya. Guzhovskiĭ, A. V. Ershov, and L. M. Lazarev, Yad. Fiz. **46**, 499 (1987) [Sov. J. Nucl. Phys. **46**, 269 (1987)].
[13] S. N. Abramovich, B. Ya. Guzhovskiĭ, and L. M. Lazarev, in *Program and Abstracts of Papers at the 35th Symposium on Nuclear Spectroscopy and Nuclear Structure* [in Russian] (Nauka, Leningrad, 1985), p. 546.
[14] C. A. Barnes, in *Nuclear Isospin, Proc. Conf.*, Asilonar, California, No. 4 (Academic Press, 1969), p. 179.
[15] D. R. Goosman and P. A. Gorodetsky, Bull. Amer. Phys. Soc. **19**, 432 (1974).
[16] A. Bohr and B. R. Mottelson, *Nuclear Structure*, Vol. 1 (Benjamin, New York, 1969) [Russ. transl., Mir, Moscow, 1971].
[17] M. Cenja, M. Duma, C. Hategan *et al.*, Izv. Akad. Nauk SSSR, Ser. Fiz. **47**, 2143 (1983); M. Cenja, M. Duma, C. Hategan, and M. Tanase, Nucl. Phys. **A307**, 65 (1978).
[18] A. S. Deineko, J. J. Malakhov, V. E. Storyzko *et al.*, Phys. Lett. **87B**, 32 (1979).
[19] A. M. Lane, Phys. Lett. **33B**, 274 (1970); R. H. Fulmer, A. L. McCarthy, B. L. Cohen, and R. Middleton, Phys. Rev. **133**, B955 (1964).
[20] P. Richard, in *Nuclear Isospin, 1969, Proc. of the Conf. on Nuclear Isospin*, Asilonar, California (1969), p. 535; E. R. Gosman, H. A. Enge, and A. Sperduto, Phys. Rev. **165**, 1175 (1968).
[21] M. F. Andreev, Yu. M. Bol'shakov, V. V. Gladkov *et al.*, Yad. Fiz. **51**, 942 (1990) [Sov. J. Nucl. Phys. **51**, 603 (1990)].
[22] S. Bjornholm and J. E. Lynn, Rev. Mod. Phys. **52**, 725 (1980).
[23] A. M. Lane and R. G. Thomas, Rev. Mod. Phys. **30**, 257 (1958) [Russ. transl., IL, Moscow, 1960]; E. P. Wigner and L. Eisenbud, Phys. Rev. **72**, 29 (1947).
[24] C. Hategan, Ann. Phys. (N.Y.) **116**, 77 (1978); M. S. Ama, C. Hategan, and N. A. Shlyakhov, Izv. Akad. Nauk SSSR, Ser. Fiz. **48**, 366 (1984).
[25] L. M. Lazarev, Ukr. Fiz. Zh. **36**, 661 (1991).
[26] H. M. Hoffmann, Nucl. Phys. **A416**, 363 (1984).
[27] P. L. Kapur and R. E. Peierls, Proc. R. Soc. Ser. A **166**, 277 (1938).
[28] L. M. Lazarev, Izv. Akad. Nauk SSSR, Ser. Fiz. **39**, 2104 (1975); Yad. Fiz. **23**, 735 (1976) [Sov. J. Nucl. Phys. **23**, 387 (1976)].
[29] M. A. Preston, *Physics of the Nucleus* (Addison-Wesley, Reading, Mass., 1962) [Russ. transl., Mir, Moscow, 1964].
[30] A. S. Davydov, *Theory of the Nucleus* [in Russian] (Fizmatgiz, Moscow, 1958), Chaps. 8–9.
[31] V. V. Anisovich and A. A. Ansel'm, Usp. Fiz. Nauk **88**, 287 (1966) [Sov. Phys. Usp. **9**, 117 (1966)].
[32] E. W. Schmid and H. Ziegelman, *The Quantum Mechanical Three-Body Problem* (Pergamon Press, Oxford, 1974) [Russ. transl., Nauka, Moscow, 1979], Chap. 4.
[33] L. M. Lazarev, Yad. Fiz. **6**, 416 (1967) [Sov. J. Nucl. Phys. **6**, 301 (1968)].
[34] L. M. Lazarev, Yad. Fiz. **5**, 101 (1967) [Sov. J. Nucl. Phys. **5**, 69 (1967)].
[35] A. B. Volkov, Nucl. Phys. **74**, 33 (1965).
[36] F. Tanabe, A. Tashaki, and R. Tamagaki, Prog. Theor. Phys. **53**, 677 (1975).
[37] V. S. Vasilevskiĭ, T. P. Kovalenko, and G. F. Filippov, Yad. Fiz. **48**, 346 (1988) [Sov. J. Nucl. Phys. **48**, 217 (1988)].
[38] D. Halderson, M. Yu, and Y. Yu, Phys. Rev. C **39**, 336 (1989).
[39] I. F. Gutich and I. P. Okhrimenko, Yad. Fiz. **47**, 1238 (1988) [Sov. J. Nucl. Phys. **47**, 788 (1988)].
[40] G. Bluge, K. Langanke, M. Plagge *et al.*, Phys. Lett. **238**, 137 (1990).
[41] M. Bruno, F. Cannata, M. D'Agostino *et al.*, Nucl. Phys. **A501**, 462 (1989).
[42] L. L. Chopovskiĭ, Yad. Fiz. **50**, 1329 (1989) [Sov. J. Nucl. Phys. **50**, 824 (1989)]; Nucl. Phys. **A500**, 140 (1989).
[43] Yu. A. Simonov, Yad. Fiz. **22**, 845 (1975) [Sov. J. Nucl. Phys. **22**, 437 (1975)].
[44] Yu. A. Simonov, Zh. Eksp. Teor. Fiz. **69**, 1905 (1975) [Sov. Phys. JETP **42**, 966 (1975)].
[45] R. Blankenbecler, M. L. Goldberger, N. N. Khuri, and S. B. Treiman, Ann. Phys. (N.Y.) **10**, 62 (1960).
[46] A. G. Sitenko, *Scattering Theory* [in Russian] (Vyshcha Shkola, Kiev, 1975), Chap. 10, p. 161.
[47] É. I. Dubovoĭ, Yad. Fiz. **20**, 900 (1974) [Sov. J. Nucl. Phys. **20**, 479 (1975)].
[48] É. I. Dubovoĭ and G. I. Chitanava, Yad. Fiz. **47**, 370 (1988) [Sov. J. Nucl. Phys. **47**, 233 (1988)].
[49] H. A. Bethe and F. de Hoffmann, *Mesons and Fields* (Row, Peterson and Co., Evanston, Illinois, 1955) [Russ. transl., IL, Moscow, 1957].
[50] L. D. Landau and E. M. Lifshitz, *Quantum Mechanics*, 3rd ed. (Pergamon Press, Oxford, 1977) [Russ. original, 4th ed., Nauka, Moscow, 1989].
[51] S. Brandt, *Statistical and Computational Methods in Data Analysis* (North-Holland, Amsterdam, 1970) [Russ. transl., Mir, Moscow, 1975].
[52] S. N. Abramovich, L. A. Morkin, V. I. Serov, and Yu. V. Strel'nikov, Izv. Akad. Nauk SSSR, Ser. Fiz. **51**, 930 (1987).

[53] S. N. Abramovich, A. I. Baz', and B. Ya. Guzhovskiĭ, Yad. Fiz. **32**, 402 (1980) [Sov. J. Nucl. Phys. **32**, 208 (1980)].
[54] S. N. Abramovich, B. Ya. Guzhovskiĭ, A. G. Zvenigorodskiĭ, and S. V. Trusillo, Izv. Akad. Nauk SSSR, Ser. Fiz. **37**, 1967 (1973).
[55] S. N. Abramovich, B. Ya. Guzhovskiĭ, A. G. Zvenigorodskiĭ, and S. V. Trusillo, Yad. Fiz. **30**, 1276 (1979) [Sov. J. Nucl. Phys. **30**, 665 (1979)].
[56] S. N. Abramovich, B. Ya. Guzhovskiĭ, S. A. Dunaeva *et al.*, Vopr. At. Nauki Tekh. Ser. Yad. Konst. No. 2, 14 (1985).
[57] V. I. Serov and B. Ya. Guzhovskiĭ, At. Energ. **12**, 5 (1962).
[58] F. C. Barker and G. T. Heckey, J. Phys. G **3**, L23 (1977).
[59] J. A. Nolen and F. J. P. Schiffer, Ann. Rev. Nucl. Sci. **19**, 471 (1969).
[60] A. I. Amelin, M. G. Gornov, Yu. B. Gurov *et al.*, Yad. Fiz. **52**, 1231 (1990) [Sov. J. Nucl. Phys. **52**, 782 (1990)].
[61] K. H. Wilcox, R. B. Weisenmiller, G. J. Woznik *et al.*, Phys. Lett. **59B**, 142 (1975).
[62] B. Ya. Guzhovskiĭ and L. M. Lazarev, Izv. Akad. Nauk SSSR, Ser. Fiz. **54**, 2250 (1990).
[63] B. Ya. Guzhovskiĭ, L. M. Lazarev, and A. V. Ershov, Izv. Akad. Nauk SSSR, Ser. Fiz. **52**, 61 (1988).
[64] B. Ya. Guzhovskiĭ, A. V. Ershov, and L. M. Lazarev, Izv. Akad. Nauk SSSR, Ser. Fiz. **54**, 155 (1990).
[65] L. Brown, E. Steiner, L. C. Arnold, and R. G. Seyler, Nucl. Phys. **A206**, 353 (1973).
[66] L. Arnold, R. Seyler *et al.*, Phys. Rev. Lett. **32**, 895 (1974).
[67] R. C. Seyler, Nucl. Phys. **A124**, 253 (1969).
[68] M. Laurat, CEA-R-3727, Orsay University, Paris (1969).
[69] S. N. Abramovich, B. Ya. Guzhovskiĭ, V. A. Zherebtsov, and A. G. Zvenigorodskiĭ, Vopr. At. Nauki Tekh. Ser. Yad. Konst. No. 4(58), 17 (1984).
[70] P. Darriulat, G. Igo, H. G. Pugh, and H. D. Holmgren, Phys. Rev. **137**, 315 (1965).
[71] N. Jarmie, R. E. Brown, and R. A. Hardekopf, Phys. Rev. C **29**, 2031 (1984).
[72] H. M. Hoffman, T. Mertelmeier, and W. Zahn, Nucl. Phys. **A410**, 208 (1983).
[73] T. Kajino, Nucl. Phys. **A460**, 559 (1986).
[74] B. Buck and A. C. Merchant, J. Phys. G **14**, L211 (1988).
[75] M. Haller, W. Kreischmer, and A. Rauscher, Nucl. Phys. **A496**, 190 (1989).
[76] M. Haller, W. Kreischmer, and A. Rauscher, Nucl. Phys. **A496**, 205 (1989).
[77] G. M. Ter-Akop'yan, Fam Ngok Chong, N. V. Eremin *et al.*, Preprint R15-85-775 [in Russian], JINR, Dubna (1985); N. V. Eremin, Sh. S. Zeĭnalov, A. P. Kabachenko *et al.*, in *Program and Abstracts of Papers at the 37th Symposium on Nuclear Spectroscopy and Nuclear Structure* [in Russian] (Nauka, Leningrad, 1987), p. 300.
[78] B. V. Govorov, N. V. Eremin, I. V. Tyapkin *et al.*, in *Program and Abstracts of Papers at the 41st Symposium on Nuclear Spectroscopy and Nuclear Structure* [in Russian] [Nauka, Leningrad (1991)], p. 264.
[79] G. Breit, *Theory of Resonance Nuclear Reactions* [Russian translation], (IL, Moscow, 1961).
[80] M. H. Hull and G. Breit, in *Handbuch der Physik*, Vol. **41/1** (1959), p. 408.
[81] D. A. Frank-Kamenetskiĭ, *Physical Processes Within Stars* [in Russian] (Fizmatgiz, Moscow, 1959).
[82] V. A. Tsarev, Usp. Fiz. Nauk **160**, No. 11, 1 (1990) [Sov. Phys. Usp. **33**, 881 (1990)].

Translated by Julian B. Barbour